EBioMedicine 10 (2016) 85–100

Contents lists available at ScienceDirect

EBioMedicine

journal homepage: www.ebiomedicine.com

Research Paper

# Inactivation of the CRL4-CDT2-SET8/p21 ubiquitylation and degradation axis underlies the therapeutic efficacy of pevonedistat in melanoma

Mouadh Benamar [a], Fadila Guessous [a], Kangping Du [a], Patrick Corbett [a], Joseph Obeid [b], Daniel Gioeli [c], Craig L. Slingluff Jr [b], Tarek Abbas [a,d,e,*]

[a] Department of Radiation Oncology, University of Virginia, Charlottesville, VA 22908, USA
[b] Department of Surgery, University of Virginia, Charlottesville, VA 22908, USA
[c] Department of Microbiology, Immunology, and Cancer Biology, University of Virginia, Charlottesville, VA 22908, USA
[d] Department of Biochemistry and Molecular Genetics, University of Virginia, Charlottesville, VA 22908, USA
[e] Center for Cell Signaling, University of Virginia, Charlottesville, VA 22908, USA

ARTICLE INFO

*Article history:*
Received 9 May 2016
Received in revised form 13 June 2016
Accepted 15 June 2016
Available online 16 June 2016

*Keywords:*
Melanoma
CDT2
DTL
Cullin
Ubiquitylation
MLN4924
Pevonedistat
BRAF
NRAS

ABSTRACT

The cullin-based CRL4-CDT2 ubiquitin ligase is emerging as a master regulator of cell proliferation. CRL4-CDT2 prevents re-initiation of DNA replication during the same cell cycle "rereplication" through targeted degradation of CDT1, SET8 and p21 during S-phase of the cell cycle. We show that CDT2 is overexpressed in cutaneous melanoma and predicts poor overall and disease-free survival. CDT2 ablation inhibited a panel of melanoma cell lines through the induction of SET8- and p21-dependent DNA rereplication and senescence. Pevonedistat (MLN4924), a specific inhibitor of the NEDD8 activating enzyme (NAE), inhibits the activity of cullin E3 ligases, thereby stabilizing a vast number of cullin substrates and resulting in cancer cell inhibition *in vitro* and tumor suppression in nude mice. We demonstrate that pevonedistat is effective at inhibiting the proliferation of melanoma cell lines *in vitro* through the induction of rereplication-dependent permanent growth arrest as well as through a transient, non-rereplication-dependent mechanism. CRISPR/Cas9-mediated heterozygous deletion of *CDKN1A* (encoding p21) or *SET8* in melanoma cells demonstrated that the rereplication-mediated cytotoxicity of pevonedistat is mediated through preventing the degradation of p21 and SET8 and is essential for melanoma suppression in nude mice. By contrast, pevonedistat-induced transient growth suppression was independent of p21 or SET8, and insufficient to inhibit tumor growth *in vivo*. Pevonedistat additionally synergized with the BRAF kinase inhibitor PLX4720 to inhibit BRAF melanoma, and suppressed PLX4720-resistant melanoma cells. These findings demonstrate that the CRL4-CDT2-SET8/p21 degradation axis is the primary target of inhibition by pevonedistat in melanoma and suggest that a broad patient population may benefit from pevonedistat therapy.

*Research in Context:* The identification of new molecular targets and effective inhibitors is of utmost significance for the clinical management of melanoma. This study identifies CDT2, a substrate receptor for the CRL4 ubiquitin ligase, as a prognostic marker and therapeutic target in melanoma. CDT2 is required for melanoma cell proliferation and inhibition of $CRL4^{CDT2}$ by pevonedistat suppresses melanoma *in vitro* and *in vivo* through the induction of DNA rereplication and senescence through the stabilization of the $CRL4^{CDT2}$ substrates p21 and SET8. Pevonedistat also synergizes with vemurafenib *in vivo* and suppresses vemurafenib-resistant melanoma cells. These findings show a significant promise for targeting $CRL4^{CDT2}$ therapeutically.



## 1. Introduction

Melanoma is an aggressive cancer affecting approximately 80,000 patients per year in the USA, with poor prognosis in the metastatic stage (Balch et al., 2009). It is the sixth most common fatal malignancy accounting for about 4% of all cancer-related deaths (Siegel et al., 2012). At the molecular level, activating mutations in the serine/threonine kinase BRAF (p.V600E) or NRAS (mostly p.Q61R or p.Q61K) occur in a majority (60–70%) of cases (Davies et al., 2002; Davies and Samuels, 2010). Both oncogenes activate the classical mitogen-activated protein kinase (MAPK) pathway, but NRAS additionally activates the phosphatidylinositol 3-kinase (PI3K) pro-survival pathway. The recent development of inhibitors of oncogenic BRAF, such as vemurafenib and dabrafenib, has offered significant opportunities for the treatment of at least a

* Corresponding author at: Department of Radiation Oncology, University of Virginia, Charlottesville, VA 22908, USA.
*E-mail address:* ta8e@virginia.edu (T. Abbas).

http://dx.doi.org/10.1016/j.ebiom.2016.06.023

subset of melanoma patients (Chapman et al., 2011; Flaherty et al., 2010; Hersey et al., 2009; Sosman et al., 2012). The development of therapeutic resistance however, represents major challenges that require the identification of alternative therapeutic approaches and new molecular targets and chemical inhibitors that can exert anti-melanoma activity and can operate irrespective of the *BRAF* or *NRAS* mutational status.

Polyubiquitylation leading to proteolytic degradation by the 26S proteasome is involved in all aspects of cell physiology. The highly coordinated process ensures the selective and timely turnover of proteins, thereby controlling cellular activity and maintaining cell and tissue homeostasis (Glickman and Ciechanover, 2002). The **c**ullin **4 R**ING E3 ubiquitin **l**igase (CRL4) is a master regulator of genome stability and orchestrates a variety of physiological processes, particularly those related to chromatin regulation (Jackson and Xiong, 2009). Along with the substrate receptor CDT2 (also known as DCAF2, DTL/RAMP), the $CRL4^{CDT2}$ ligase promotes the ubiquitin-dependent degradation of several proteins essential for cell cycle progression as well as for DNA replication and repair (Abbas and Dutta, 2011; Abbas et al., 2013). One of the main functions of $CRL4^{CDT2}$ is to prevent re-initiation of DNA replication (rereplication), both during S-phase of the cell cycle and following DNA damage, through the ubiquitylation and degradation of the replication licensing protein CDT1 (unrelated to CDT2), the CDK inhibitor p21, and the histone methyltransferase SET8 (Abbas and Dutta, 2011; Abbas et al., 2013). DNA rereplication is deleterious to cells and promotes cellular senescence and apoptosis due to replication fork stalling and the accumulation of toxic replication intermediates.

Cullin-dependent E3 ligases, including CRL4, are activated by NEDD8 modification, which is catalyzed by an enzyme cascade system similar to ubiquitylation (Merlet et al., 2009). Pevonedistat (MLN4924), an inhibitor of the NEDD8-activating enzyme (NAE), induces cytotoxicity in a variety of cancer cell types *in vitro* and in preclinical mouse models (Jazaeri et al., 2013; Lin et al., 2010; Soucy et al., 2009; Wei et al., 2012). It is currently in clinical trials for hematologic (NCT00722488, NCT00911066) and solid malignancies including melanoma (NCT01011530), but its effects on melanoma cells have not been thoroughly examined. There is also little to no preclinical data on pevonedistat efficacy in the context of the various genetic mutations associated with melanoma or resistance to front line therapies (Garcia et al., 2014; Tan et al., 2013). Consistent with its activity as a general inhibitor of protein neddylation, pevonedistat was shown to inhibit multiple signal transduction pathways in addition to inhibiting cullin-mediated signaling, including the NFκB, AKT and the mTOR signal transduction pathways (Godbersen et al., 2014; Gu et al., 2014; Li et al., 2014a; Li et al., 2014b; Lin et al., 2010; Milhollen et al., 2011; Milhollen et al., 2010; Soucy et al., 2009). Although pevonedistat exerts these wide inhibitory activities, it remains unclear which, if any, mediates its anti-tumor activity.

We here show that CDT2 is frequently overexpressed in melanoma, and its elevated expression predicts poor overall and disease-free survival. CDT2 knockdown or deletion inhibits the proliferation of melanoma cells *in vitro* through the induction of rereplication and senescence, and *via* a mechanism that is dependent on the stabilization of the $CRL4^{CDT2}$ substrates SET8 and p21. Pevonedistat exerts significant anti-melanoma activity, irrespective of the BRAF mutational status, and through the induction of SET8- and p21-dependent rereplication and senescence. *In vivo* studies using melanoma cells with hypomorphic expression of p21 or SET8 show that both of these proteins are required for the anti-melanoma efficacy of pevonedistat, demonstrating that inhibition of the $CRL4^{CDT2}$-SET8/p21 degradation axis is the primary mechanism by which pevonedistat inhibits melanoma. Finally, we show that pevonedistat synergizes with the BRAF kinase inhibitor PLX4720 to suppress BRAF mutant melanoma *in vivo*, and suppresses PLX4720-resistant melanoma cells.

## 2. Materials & Methods

### 2.1. Cell Culture and Reagents

VMM39, VMM1, and VMM18 human melanoma cell lines were established from metastatic lesions of patients at the University of Virginia (IRB #5202, by CLS). DM93, DM331, DM13 and SLM2 melanoma cell lines had been established from metastatic lesions by Dr. H.F. Seigler at Duke University (Hogan et al., 2005; Huntington et al., 2004; Kittlesen et al., 1998; Molhoek et al., 2008; Slingluff et al., 1993; Yamshchikov et al., 2001; Yamshchikov et al., 2005). SK-MEL-2 and SK-MEL-28 melanoma cells were established in Memorial Sloan Kettering Cancer Center and obtained from the American Type Culture Collection (ATCC, Manassas, VA). All melanoma cells were grown in RPMI media supplemented with 10% fetal bovine serum (FBS) and 1% penicillin/streptomycin (P/S). PIG1 and PIG3V melanocytes were described before (Le Poole et al., 2000) and maintained in Media 254 containing 1% of human melanocyte growth supplement (HMGS), 5% FBS and 1% (P/S). All cells were grown at 37 °C in 5% $CO_2$. Tissue extraction reagent I was obtained from Invitrogen (Carlsbad, CA). Propidium iodide, 7-AAD and BrdU kit were purchased from BD Biosciences (San Diego, CA). Vector's ImmPRESS polymer kit for TMAs immunostaining was obtained from Vector laboratories (Burlingame, CA). Pevonedistat and vemurafenib (PLX4032) were purchased from Active Biochem (Wan Chai, Hong Kong), and were dissolved in DMSO and used at the indicated doses.

### 2.2. Cell Lysis, SDS-PAGE and Immunoblotting

Melanoma cells were lysed with RIPA lysis buffer (50 mM Tris, pH 8.0; 150 mM NaCl, 1% NP-40; 0.5% sodium deoxycolate; 0.1% SDS; 1 mM Benzamidin -HCl; 0.5 μg/ml Leupeptin; 0.5 μg/ml Aprotinin; 1 μg/ml pepstatin; 20 mM NaF; 20 mM $Na_3VO_4$), and equal amounts of protein were electrophoretically separated in a polyacrylamide 8–12% gel (BioRad, Hercules, CA), trans-blotted to a nitrocellulose membrane, and incubated overnight with primary antibodies at 4 °C. The following antibodies were used: anti-p21 (C19), anti-p27 (C19), anti-p53 (DO-1), and anti-tubulin (10D8) were purchased from Santa Cruz (California). Antibodies against SET8, CHK1, CHK2, p-CHK1 (S375), p-CHK2 (T68), H2AX and p-H2AX (γH2AX; T139), and PARP were purchased from Cell Signaling (Danvers, MA). Anti-Cul3 was purchased from Bethyl Laboratories (Montgomery, TX). Anti-CDT1 and anti-CDT2 antibodies were described before (Abbas et al., 2010). The immunoblot signals were detected by enhanced chemiluminescence. For melanoma xenografts, tumors were isolated, washed three times with cold PBS and frozen at −80 °C until use. Frozen specimens were grinded in a dry-iced mortar and subsequently lysed in 2× volume of tissue extraction reagent I, supplemented with protease and phosphatase inhibitors as stated above. Tissue lysates were probed for different proteins by immunoblotting following the procedure described above.

### 2.3. RNA Interference (siRNA)-Mediated Gene Silencing

si-RNA transfections were performed using lipofectamine RNAimax according to the manufacturer's protocol (Invitrogen, Carlsbad, CA). Cells were seeded at 30% confluency and transfected with the individual siRNAs (10 nM each) in RPMI media supplemented with 10% fetal bovine serum (FBS) and 1% penicillin/streptomycin (P/S). In co-knockdown experiments, DM93 or VMM39 cells were transfected with the individual siRNAs (10 nM each with 10 nM control siGL2-for normalization) or siRNAs targeting CDT1, SET8 or p21 along with siRNA targeting CDT2 (10 nM each – total 20 nM siRNAs). Control cells were transfected with 20 nM si-GL2. Cells were harvested 72 h post-transfection for cell cycle analysis or at 96 h for β-gal staining. The following siRNAs were used (sense strand): si-GL2: 5′-AACGUACGCGGAAUACUUCGA-3′; si-CDT2: 5′-GAAUUAUACUGC UUAUCGA-3′, si-CDT1: 5′-AACGUGGAUGAAGUACCCGAC-3′; si-

SET8: 5′-GAUUGAAAGUGGGAAGGAA-3′; si-p21: 5′-AACAUACUG GCCUGGACUG-3′; si-Geminin: 5′-UGCCAACUCUGGAAUCAAA-3′. si-EMI1 were described previously (Machida and Dutta, 2007).

### 2.4. Gene Targeting by CRISPR/Cas9

Single guide-RNAs (sgRNAs) targeting the *DTL* (sg-CDT2-1 and sg-CDT2), *SET8* and *CDKN1A* genes were cloned into pX330 vector containing a human codon-optimized *Sp*Cas9 endonuclease (Addgene #42230) using BbsI restriction enzyme cutting sites, and transfected in the various cell lines. After puromycin selection, cells were seeded to obtain single colonies. Genomic DNA was extracted using 100 mM NaCl, 50 mM Tris-HCl pH 7.0, 5 mM EDTA and 1% SDS. Genotyping was performed using PCR amplification of genomic DNA using the following forward and reverse primer sets, respectively. For CDT2: 5′-TGTTGTGAGAGGCGCAAGCTGC-3′ and 5′-GGTCGGAGGTGGCGTGTGTTTC-3′; for SET8: 5′-GTCTTTCCCCCACC TCCGCCTG-3′ and 5′-CTTTTTTCGGGGGGCCTGTTTGC-3′; for p21: 5′-TCACCTGAGGTGACACAGCAAAGC-3′ and 5′-GGCCCCGTGGGAAG GTAGAGCTT-3′. Targets of the various sgRNAs are as follows: For *DTL* (*CDT2*): 5′-GCACCGAATTGAAGAGCATC-3′ (for sg-CDT2-1); and 5′-CATTTCTCAGGACGCCAAGC-3′ (for sg-CDT2-2); for *SET8*: 5′-ACGGAGCGCCATGAAGTCCG-3′; for *CDKN1A*: 5′- GCGCCATGT CAGAACCGGCT-3′. Insertions/deletions (Indels) identification was performed using Surveyor Mutation Detection Kit according to the manufacturer's protocol (Integrated DNA Technologies, CA). For sequencing, PCR amplified gene products were cloned into Topo TA Vector using TOPO TA cloning Kit according to the manufacturer's protocol (Invitrogen, CA) and transformed into DH5α. Plasmids were retrieved by the QIAprep Spin Miniprep Kit (Qiagen) and confirmed by sequencing (Eurofins Scientific).

### 2.5. Cell Proliferation/Viability Assays and Washout Experiments

Proliferation/viability of cultured cells was measured by CellTiter96 Non-radioactive cell proliferation assay (Promega; Madison, WI). Briefly, various wild type and mutant BRAF melanoma cells were seeded in 96 well plates and treated with pevonedistat, vemurafenib or the combination pevonedistat and vemurafenib at various concentrations. Control cells were treated with DMSO. 96 h following treatment, cells were stained with the dye solution according to the manufacturer's protocol. Absorbance was recorded at 570 nm and growth curves were established. To test the effect of transient exposure of melanoma cells to pevonedistat on rereplication and growth inhibition, we conducted the washout experiments where melanoma cells or PIG3V melanocytes were treated with 1 μM pevonedistat for different times (4, 8, 12 and 24 h) before the drug was washed out by washing the cells 2× with PBS, and adding drug-free fresh growth media to cells. Cells were counted every 24 h by Countess Automated Cell Counter (Invitrogen), and harvested at the indicated times for PI staining and FACS analysis (cell cycle profile) or for immunoblotting.

### 2.6. Clonogenic Survival Assays

Cell survival following CDT2 depletion or pevonedistat treatment was assessed by clonogenic survival assay, preformed in triplicates. 72 h following transfection with si-GL2 or si-CDT2, cells were trypsinized, counted and seeded in 60 mm dishes. For pevonedistat treatments, cells were counted and seeded in 60 mm dishes and treated 24 h later with various doses of pevonedistat or with DMSO. Cells were cultured for two weeks and were subsequently washed in cold PBS, fixed in cold methanol for 10 min and stained with crystal violet (0.5%) for 10 min. Plates were washed with water, dried and pictures were captured using Imagelab software (BioRad). Quantification of colonies was performed using QuantityOne software (BioRad). Results are represented as mean ± s.e.m. of triplicates normalized to the corresponding DMSO-treated or si-GL2 transfected controls.

### 2.7. Senescence-Associated β-galactosidase Assays

Senescence was monitored using β-galactosidase (β-gal) staining. Following the various treatments, cells were washed twice with PBS, fixed with 2% formaldehyde/0.2% gluteraldehyde in PBS for 15 min at room temperature, and washed 2× with PBS. The cells were stained with fresh X-Gal solution (1 mg/ml X-gal, 40 mM $C_6H_8O_7 \cdot H_2O$, 5 mM $K_3Fe(CN)_6$, 5 mM K4Fe$(CN)_6 \cdot 3H_2O$, 150 mM NaCl, and 2 mM $MgCl_2 \cdot 6H2O$ in PBS) for 3–12 h at 37 °C in the dark. Cells were washed 3× in PBS and fixed with 100% methanol for 5 min at room temperature. Bright field blue color images were taken with an AMG EvosXL Core Imager/camera microscope, counting at least 100 cells from at least 3 fields.

### 2.8. Flow Cytometry Analysis

The effects of pevonedistat, vemurafenib and/or silencing of various cell cycle-associated proteins by siRNA on cell cycle distribution and rereplication were assessed by propidium iodide staining and flow cytometry of asynchronous melanoma cultures. Synchronization of cells was not employed to avoid bias and to be able to measure the impact of these perturbations on proliferating cancer cells. Briefly, asynchronous melanoma cell lines were treated with pevonedistat or vemurafenib, or transfected with si-CDT1, si-CDT2, si-SET8, si-p21, si-geminin, si-EMI1 or si-GL2 for a time ranging from 24 to 96 h. Cells were washed with cold PBS, harvested, and fixed in 70% (v/v) ethanol. Cells were subsequently treated with 20 μg of DNase-free RNase and stained with propidium iodide according to instructions of the manufacturer. Samples were analyzed on a FACscan (Becton Dickinson) and $G_0$-$G_1$, S, and $G_2$-M fractions were segmented, and apoptotic (sub-G1 DNA content) and rereplicating (>G2/M DNA content) fractions were determined using FlowJo and ModFit softwares.

### 2.9. Bromodeoxy Uridine (BrdU) Staining and Flow Cytometry

The effects of pevonedistat and/or silencing of cell cycle-associated proteins on cell cycle distribution or rereplication were assessed by flow cytometry according to the manufacturer's instructions. Different melanoma lines were transfected with si-GL2, si-CDT2, si-CDT1, si-SET8, si-p21 or si-geminin for a time ranging from 24 to 96 h. At the end of treatment, cells were pulsed with BrdU (10 nM) for 1 h in the dark prior to harvesting. Cells were washed with PBS and staining solution before the fixation and permeabilization steps according to the manufacturer's instructions. Cells were subsequently stained with anti-BrdU antibody solution for 20 min at room temperature, washed and stained with 7-AAD solution for 30 min at 4 °C. The cells were resuspended in 1 ml of staining buffer and kept overnight at 4 °C before analysis. Samples were analyzed on a FACscan (Becton Dickinson), and different phases of the cell cycle were determined using FlowJo and ModFit softwares.

### 2.10. Staining and Analysis of Melanoma Tissue Microarray (TMA)

Formalin-fixed paraffin-embedded (FFPE) tissue blocks were retrieved from archives of the Department of Pathology, University of Virginia. Use of human tissues was approved by the UVA Institutional Review Board (protocol 10598). Hematoxylin and eosin (H&E) slides from each block were reviewed by a pathologist (JS) to identify tumor areas. TMAs were constructed with 1.0-mm diameter tissue cores from representative tumor areas from the FFPE tissue blocks, transferred into a recipient paraffin block using a semi-automated tissue array instrument (TMArrayer; Pathology Devices). Quadruplicate or triplicate tissue cores were taken from each specimen, resulting in 9

composite TMA blocks containing tissue cores from 18 to 27 specimens each. Control tissues from spleen, liver, placenta, and kidney were included in each TMA block (not shown). Multiple 4 μm sections were cut for H&E and immunohistochemical staining. The human melanoma tissue microarray (TMA) was evaluated for expression of CDT2 and Ki67 by immunohistochemistry. Details of this TMA have been reported previously (Erdag et al., 2012). These arrays included surgical specimens of human melanoma. Protein expression patterns of CDT2 and Ki67 were assessed in 138 tumor specimens in the TMA. Three nevi were used as a control. Antigen-retrieval step was performed at low pH 0.01% citric acid for 20 min at 100 °C. Endogenous peroxidase was blocked using Vector's Bloxall (SP-6000) for CDT2 detection and 0.3% Hydrogen peroxide for Ki67 detection; for 10 min; prior to serum blocking for 20 min, at room temperature. Incubation with CDT2 primary antibody (Abbas et al., 2008) (1:100 dilution) was performed at room temperature for 30 min. Staining with Ki67 primary antibody (Vector laboratories; 1:50 dilution) was performed overnight at 4 °C. Omitting the primary antibody served as a negative control for the staining. The Secondary antibody (SK-4200 ImmPRESS reagent; 1:500 dilution) was used for 30 min followed by substrate AEC (Vector laboratories) incubation for 20 min, at room temperature as per the kit's instructions. Diaminobenzidine was utilized as the final chromogen and hematoxylin as the nuclear counterstain. Staining frequency of CDT2 and Ki67 were quantified manually by counting the number of positively stained nuclei in an average of three fields per core. The frequency is calculated by dividing the number of positive staining over the total number of cells in the same fields.

Immunohistochemical staining for BRAF mutation (V600E) was performed at the University of North Carolina, using Leica's Bond autostainer (Leica Biosystems, Nussloch, Germany) and the BRAF V600E antibody (Spring Bioscience, clone VE1, dilution 1:400). Mutational status is assessed by the presence or absence of staining in each core. Tumors with borderline staining and those with discrepant expression in between cores were excluded. The consensus value of the 2–4 representative cores from each tumor/patient sample arrayed was used for scoring and statistical analyses. TMA slides were quantified using Aperio ImageScope V11.2.

### 2.11. Kaplan-Meier Plot Analysis

Publicly available TCGA data at cBioPortal (Cerami et al., 2012; Gao et al., 2013) was used to plot Kaplan-Meier plots on tumors divided into two groups based on level of CDT2 expressed as a Z-score (Collisson et al., 2014; Taylor et al., 2010; Weinstein et al., 2014).

### 2.12. Tumor Xenograft Studies

Animals were housed and handled in accordance with the guidelines of the Animal Care and Use Committee (ACUC) of the University of Virginia. The effect of pevonedistat on melanoma growth was tested in flank xenograft models. Foxn1$^{nu}$ (20–25 g body weight, 4–5 weeks old females) athymic nude immune-deficient mice (Harlan laboratories) were used in this study. Pevonedistat was dissolved in sterile 10% DMSO containing PBS (stock 1 mM) and stored in −20 °C until use. $2 \times 10^6$ of DM93, VMM39, SLM2, DM331 or SK-MEL-24 melanoma cells were implanted in both flanks of immune-deficient mice ($n = 12$ mice per group) and tumor growth was monitored until reaching an average volume of 150–200 mm$^3$. Mice were randomized into groups for treatment. Animals were administered 0.2 mL pevonedistat solution (30 or 60 mg/kg body weight as indicated) intraperitoneally on a schedule of two cycles of five-day treatment followed by five treatment-free days, for a total of 3 weeks, or more as indicated. Control animals were treated with an equal volume of sterile vehicle (10% DMSO in PBS). Where indicated, mice received control rodent diet, or diet with 417 mg/kg PLX4720 (Research Diets, Inc. New Brunswick, NJ). Tumors were measured with an electronic caliper every other day for 3 weeks post-drug injection. Animal weight was recorded once a week to detect any weight loss due to the toxicity of drug treatment or tumor burden. At the end of treatment, animals were euthanized and tumors harvested for further processing. The results shown are mean tumor volumes at the indicated time ± s.e.m.; $^*p < 0.05$, $^{**}p < 0.01$, $^{***}p < 0.001$.

### 2.13. Statistical Analysis

All experiments were performed in triplicates. Numerical data were expressed as mean ± standard deviation (SD). Where applicable, data are presented as the mean ± s.e.m. Two group comparisons were analyzed by two-sided Student's *t*-test. *P*-values were determined for all analyses and $p < 0.05$ was considered significant. Synergy was determined using the Bliss model of independence (Bliss, 1939; Fitzgerald et al., 2006). For correlations, a Spearman correlation was used and *p*-values <0.05 were considered statistically significant.

## 3. Results

### 3.1. CDT2 Is Overexpressed in Melanoma and Its Elevated Expression Predicts Poor Patient Outcome

Melanoma is a malignancy in which genetic predisposition is, to a large extent, associated with mutations in genes controlling DNA replication and/or proliferation (*e.g. CDKN2A*), but thus far most successful targeted drugs have focused on the oncogenic drivers in the MAP Kinase pathway (Lovly and Shaw, 2014). We suspected that vulnerabilities to drugs targeting the DNA replication machinery would be identified, and thus, searched gene expression databases for alterations in genes controlling DNA replication in melanoma. Using mRNA expression in a publicly available database of cutaneous melanomas (Talantov et al., 2005), we found that CDT2 is overexpressed in 84% of melanomas compared with normal skin or with benign skin nevi (Fig. 1a and b). CDT2 was also overexpressed in breast, cervical, gastric, lung, pancreatic, and brain malignancies (Figure S1). CDT2 overexpression in melanoma was specific, as we did not detect changes in the expression of Cul4A, Cul4B, RBX1, or 4 other DCAFs *i.e.* DDB2, VPRBB1, DWR68 and DCAF8 (Figure S2a).

We also examined the expression of CDT2 in melanoma using data obtained from The Cancer Genome Atlas (TCGA) project comprised of 471 primary and metastatic melanomas from 468 patients, available at cBioPortal (Cerami et al., 2012; Gao et al., 2013). Kaplan-Meier plots revealed that tumors with higher CDT2 expression correlated with significantly lower probability of overall and disease-free survival (Fig. 1c and d). DNA sequences are available for a subset (~60%, 278 samples) of this data set, which exhibited similar correlations (Figure S2b and S2c). Analysis of the *BRAF* or *NRAS* mutations in these tumors showed modest increase in the probability of overall survival in patients with *BRAF* mutations, and no significant correlations in patients with *NRAS* mutations (Figure S2d and S2e). Further analysis demonstrated that 72% of tumors with high CDT2 expression harbored either *BRAF* (31%) or *NRAS* (41%) mutations (Fig. 1e). This was not significantly different in low CDT2 expressing tumors with 74% of these tumors containing *BRAF* (52%) or *NRAS* (21%) mutations. Gene co-expression analysis demonstrated that CDT2 elevated expression correlated with the expression of several E2F1 target genes (data not shown), suggesting that CDT2 overexpression in melanoma may be due to increased E2F1 transcriptional activity, which has been shown to promote transcription from the *CDT2* (*DTL*) promoter (Nakagawa et al., 2008).

We next examined CDT2 protein expression in a human tissue microarray (TMA) comprising 138 melanoma specimens from 100 patients (42 female, 58 male, ages 23–90; mean 59 ± 16). These include 8 patients with large primary cutaneous melanoma and 92 with one or more metastatic melanomas. CDT2 protein was predominantly nuclear and significantly elevated in 84.7% of all melanomas (117/138), whereas CDT2 was not detectable in non-malignant

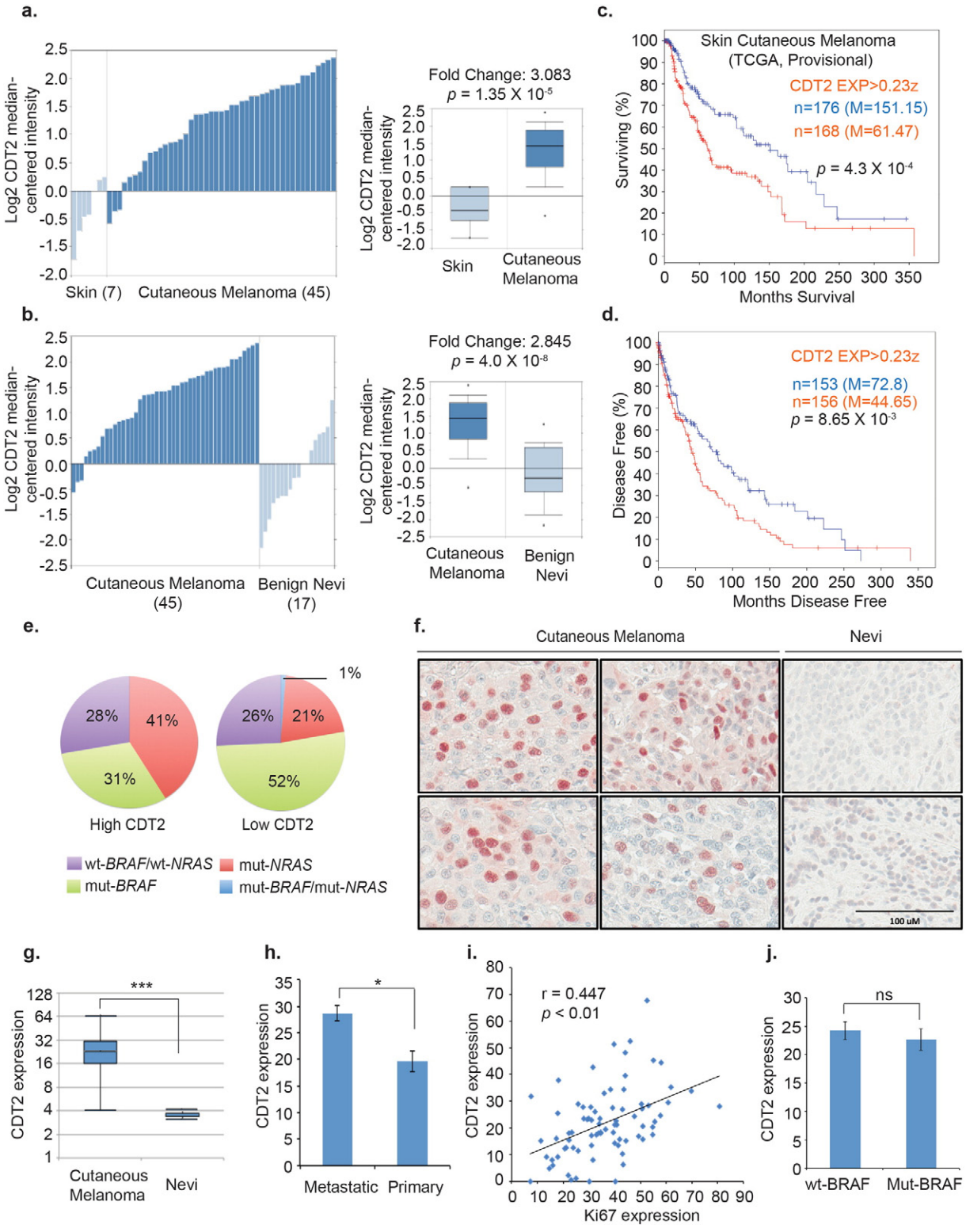


**Fig. 1.** CDT2 is overexpressed in primary and metastatic cutaneous melanoma and is a negative prognostic factor (see also Figures S1 and S2). a–b. CDT2 mRNA expression is elevated in melanoma compared to normal skin (a) or benign nevi (b). c–d. Kaplan–Meier plot of overall survival (c) or disease-free survival (d) for the human skin cutaneous melanoma (SKCM) from TCGA stratified by CDT2 median expression level. High: CDT2 level > 0.23z and Low: CDT2 level < 0.23z. EXP: the CDT2 expression level z-score cut-off used for dividing high from low expressers. n = number of patients in that group. M = median survival in months of that group (for overall survival) or median disease-free survival in months (for disease-free survival). e. Pie chart depicting the percentage of *BRAF* and *NRAS* mutations (or both) in a subset of high and low CDT2 expressing melanoma samples (in c–d) for which mutational analysis is available. f. Representative images of CDT2 staining in melanoma TMA or in melanocytic sample. Scale bar, 100 μm. g. CDT2 composite expression score in cutaneous melanoma TMA (138 melanoma specimens from 100 patients) compared to non-malignant melanocytes. ***$p < 0.001$, calculated using Student's *t*-test. h. Relative CDT2 composite expression score in metastatic melanoma compared to primary melanoma. *$p < 0.05$. i. Correlation between elevated CDT2 composite expression with Ki67 staining in the TMA analyzed in (g). j. CDT2 composite expression score in cutaneous melanoma with or without *BRAF* mutations in the TMA analyzed in (g). ns: non-significant.

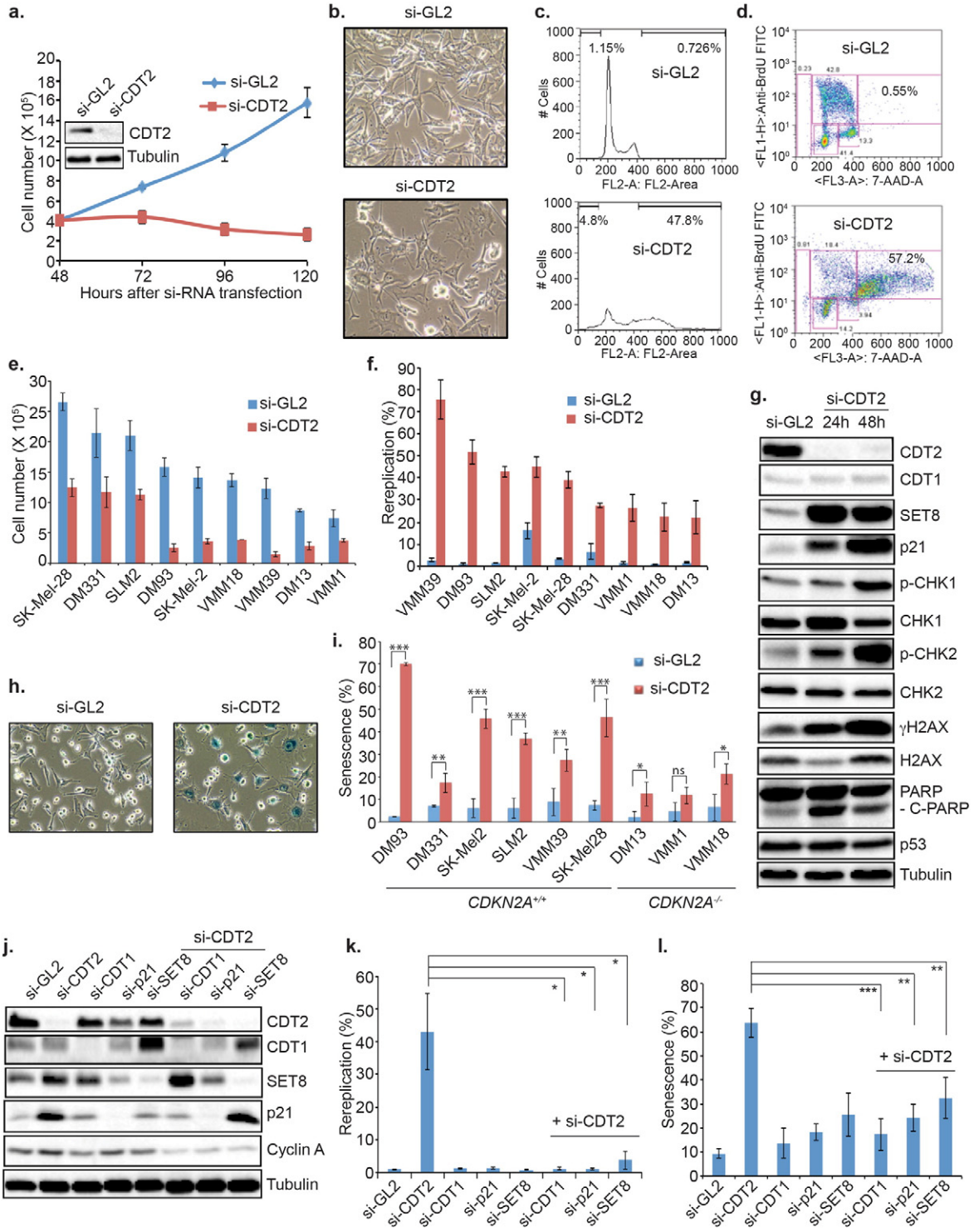


**Fig. 2.** Depletion of CDT2 inhibits melanoma cell proliferation through the induction of rereplication and senescence (see also Figures S3 and S4). a. Impact of CDT2 depletion by siRNA on the proliferation of DM93 melanoma cells. Data represent the average of three independent experiments ± S.D. (error bars). Inset: Western blot of cell lysates extracted from transfected DM93 cells and probed with the indicated antibodies. b. Representative phase contrast images depicting morphological changes in DM93 depleted of CDT2. c. Cell cycle distribution of control or si-CDT2 transfected DM93 cells as demonstrated by propidium iodide staining and FACS analysis. d. BrdU incorporation and FACS analysis demonstrating the BrdU incorporation and cell cycle distribution of DM93 cells following CDT2 depletion by siRNA. e. Graph showing the number of cells from the indicated melanoma lines 96 h following transfection with si-CDT2 or control si-GL2. $4 \times 10^6$ cells of each cell line were seeded at the beginning of transfection. Data represent the average of three independent experiments ± S.D. (error bars). f. Same as in (e) except cells were harvested at 72 h post-transfection and analyzed by FACS for DNA content. Data represent the average of three independent experiments ± S.D. g. Immunoblotting of protein lysates extracted from control or CDT2-depleted DM93 cells for the indicated time points and probed for the indicated proteins. Tubulin is loading control. C-PARP: cleaved PARP protein. h. Representative images of control or CDT2-depleted DM93 cells and stained with β-gal to detect senescence. i. The percentage of melanoma lines undergoing senescence (β-gal staining) 96 h following transfection with control (si-GL2) or CDT2 siRNA (siRNA). Data represent the average of three independent experiments ± S.D. $^*p < 0.05$ $^{**}p < 0.01$, $^{***}p < 0.001$, calculated using Student's *t*-test. ns: non-significant. j. Immunoblotting of lysates extracted from DM93 cells transfected with the indicated si-RNA and probed with the indicated antibodies. k. Percentage of rereplicating cells following the indicated treatment as determined by BrdU labeling and FACS analysis (shown in Figure S4a). Data represent the average of three independent experiments ± S.D. $^*p < 0.05$, calculated using Student's *t*-test. l. Percentage of senescent DM93 cells (β-gal staining) treated with the indicated si-RNA. Representative images are shown in Figure S4c. Data represent the average of three independent experiments ± S.D. $^{**}p < 0.01$, $^{***}p < 0.001$, calculated using Student's *t*-test.

melanocytes (Fig. 1f, g and Figure S2f). CDT2 protein expression was significantly higher in metastatic melanomas compared to primary tumors (Fig. 1h). Analysis of Ki67 staining demonstrated a statistically significant correlation between CDT2 and Ki67 staining ($r = 0.447$, $p < 0.01$) (Fig. 1l and Figure S2f). In this *in situ* analysis, we did not observe correlation between CDT2 expression and the *BRAF* mutational status, disease stage or with lymphocytic infiltration, nor did we find correlation with other parameters such as age, tissue type, gender, or patient survival (Fig. 1j, Figure S2g and S2h, and data not shown). The lack of correlation with patient survival in this dataset can be explained by the small sample size and by the fact that these tumors were mostly metastatic. Together, these results demonstrate that CDT2 expression is elevated in melanoma and serves as a negative prognostic marker for the disease.

### 3.2. CDT2 Is Required for Melanoma Cell Proliferation

Although CDT2 is overexpressed in melanoma and in other cancers, it is not likely to function as a classical oncogene. Instead, it appears to act as a cancer-associated gene to which cancer cells become "addicted". This is reminiscent to the secondary physiological changes that stress cellular capacity for survival as a consequence of oncogenic activation, common in melanoma and in other cancers; the so called "non-oncogene addiction" (Luo et al., 2009). We hypothesized that CDT2 is overexpressed in melanoma cells to alleviate replication stress that may be induced by melanoma oncogenes. To test this hypothesis, we silenced the expression of CDT2 by siRNA in a panel of melanoma lines with various genetic mutations including the BRAF mutant DM93 cells (Table S1). Depletion of CDT2 by siRNA (Fig. 2a and Figure S3a) suppressed melanoma cell proliferation and induced morphological changes associated with rereplication; flattening of cells and increase in nuclear size (Fig. 2b and e). Flow cytometry analysis confirmed the increase in cells with >4 N DNA content, the extent of which varied from cell line to cell line (Fig. 2c–f). We also detected a small but reproducible increase in cells with sub-G1 DNA content (~5% on average), indicative of apoptosis (Fig. 2c). Bromodeoxy uridine (BrdU) incorporation and FACS analysis further illustrated that CDT2 knockdown resulted in rereplication (~57%) during the same cell cycle (Fig. 2d). DNA rereplication, morphological changes and suppression of proliferation were also observed in 5 melanoma lines, including the VMM39 cells with *NRAS* and *PDGFRA* activating mutations, following the deletion of *CDT2/DTL* gene using CRISPR/Cas9 and two different single guide RNAs (sg-RNAs) that target two different regions in exon 1 of the *CDT2* gene (Figure S3b–S3e).

CDT2 knockdown in DM93, and in other melanoma cells, increased the steady state level of the $CRL4^{CDT2}$ ubiquitylation substrates SET8 and p21, but elevated CDT1 was only noted in some, but not all, melanoma lines (Fig. 2g and Figure S3a). This was associated with spontaneous DNA damage (increased γH2AX), induction of DNA damage checkpoint (phosphorylation of the checkpoint proteins CHK1 and CHK2), senescence (β-galactosidase (β-gal) staining), as well as a small increase in apoptosis (PARP cleavage) (Fig. 2g–i and Figure S3a). Thus, CDT2 depletion or deletion inhibits melanoma with various genetic mutations and this is accompanied by DNA rereplication, spontaneous DNA damage and senescence.

### 3.3. SET8 and p21 Promote Rereplication and Senescence in CDT2-Depleted Melanoma Cells

To investigate the mechanism by which CDT2 depletion induces rereplication and senescence in melanoma cells, we co-knockdown, by siRNA, the expression of various substrates of $CRL4^{CDT2}$ previously implicated in promoting DNA rereplication (Abbas and Dutta, 2011; Abbas et al., 2013) along with CDT2 in DM93 or in VMM39 cells. Knockdown of CDT1 prevented both rereplication and senescence induced by CDT2 depletion, but increased the percentage of cells in G1 and decreased S-phase cells (Fig. 2j–l, Figure S4, and data not shown), suggesting that inhibition of rereplication is secondary to cell cycle block in G1. Depletion of SET8 or p21 on the other hand, completely suppressed si-CDT2-induced rereplication, and senescence without significantly impacting cell cycle distribution (Fig. 2j–l and Figure S4). Thus, CDT1, SET8 and p21 are all required for si-CDT2-induced rereplication and senescence, but CDT1 appears to be required primarily for entry into S-phase.

To examine the role of CDT1 further, we depleted various melanoma lines (DM93, VMM39 or VMM18) of geminin, an inhibitor of CDT1 whose depletion induces rereplication in a number of cancer cell lines (Zhu and Depamphilis, 2009). Interestingly, although si-geminin efficiently induced rereplication in the U2OS osteosarcoma cells and in the Cal27 squamous cell carcinoma cells, it failed to do so in melanoma cells (Fig. 3a–c). Depletion of EMI1, an inhibitor of the APC ubiquitin ligase whose depletion results in the ubiquitin-dependent proteolysis of geminin and cyclin A (Machida and Dutta, 2007), on the other hand, induced robust rereplication in melanoma cells (Figure S5a–S5c). Thus, cyclin A, a cofactor required for CDT1 ubiquitylation *via* the $SCF^{SKP2}$ ubiquitin ligase in S-phase (Abbas and Dutta, 2011; Abbas et al., 2013), appears to restrain CDT1 activity in melanoma cells. Consistent with this hypothesis, overexpression of $SCF^{SKP2}$-resistant mutant of CDT1 ($CDT1^{\Delta CY}$), but not $CRL4^{CDT2}$-resistant mutant ($CDT1^{\Delta PIP}$; (Senga et al., 2006)), in DM93 induced rereplication more robustly than wt CDT1 (Fig. 3d, e, and Figure S5d and S5e). Thus, in melanoma cells, the steady state level of CDT1 is regulated primarily by cyclin A-mediated and $CRL1^{SKP2}$-dependent pathway.

Unlike the case for CDT1 however, the stable overexpression of wt SET8 (or p21) in DM93 or VMM39 cells did not induce rereplication (Fig. 3f, g, Figure S5f, and data not shown). In contrast, expression of SET8 mutant protein that cannot associate with PCNA ($SET8^{\Delta PIP}$) and is thus resistant to $CRL4^{CDT2}$ degradation (Abbas et al., 2010) induced rereplication in both lines, and this required SET8 catalytic activity (Fig. 3f–g, and Figure S5f–S5h). We noted that the catalytically inactive mutant of $SET8^{\Delta PIP}$ ($SET8^{\Delta PIP\text{-}CD}$) was less stable than the catalytically active protein (Fig. 3f), and its overexpression from a higher titer virus relative to catalytically active $SET8^{\Delta PIP}$ did not induce rereplication either (Figure S5g and S5h). Ectopic expression of $CRL4^{CDT2}$-resistant p21 protein ($p21^{\Delta PIP}$; (Abbas et al., 2008)) on the other hand, was associated primarily with growth arrest in early- and mid S-phase (Fig. 3f, g, and Figure S5f). Simultaneous expression of $SET8^{\Delta PIP}$ and $p21^{\Delta PIP}$ caused more rereplication in DM93 (~46% compared to ~27% with $SET8^{\Delta PIP}$ alone), but not in VMM39 cells (Fig. 3f–g, and Figure S5f). The lack of additive effects in VMM39 cells can be explained by the robust intra-S-phase cell cycle arrest caused by $p21^{\Delta PIP}$ expression in this line, preventing further rereplication. Finally, the expression of catalytically active $SET8^{\Delta PIP}$ or $p21^{\Delta PIP}$ induced senescence in both melanoma cell lines (Fig. 3h and i). Thus, deregulated SET8 expression appears to be both required and sufficient to promote rereplication and senescence in CDT2-depleted melanoma cells.

### 3.4. Pevonedistat Inhibits Melanoma Cells Through The Induction of Rereplication and Senescence, and Elevated CDT2 Expression Renders Melanoma Cells Susceptible to Pevonedistat-Induced Rereplication

The $CRL4^{CDT2}$, similar to all cullin-based ligases, is regulated by NEDD8 modification, which is catalyzed by an enzyme cascade system similar to ubiquitylation (Merlet et al., 2009). Pevonedistat inhibits cullin signaling, offering a pharmacological approach for targeting melanoma potentially through inhibiting $CRL4^{CDT2}$ ligase activity. To test this possibility, we treated DM93 cells with increasing doses of pevonedistat for 24 h. This resulted in a dose-dependent increase in several cullin ubiquitylation substrates, including CDT2, CDT1, p21 and p27, which reached significant levels at 1 μM drug concentration (Fig. 4a). Although CDT2 is increased by pevonedistat, it is likely to be inactive because of the de-neddylation of cullin proteins (Fig. 4a and b). Time course analysis with 1 μM pevonedistat demonstrated early (at 3 and

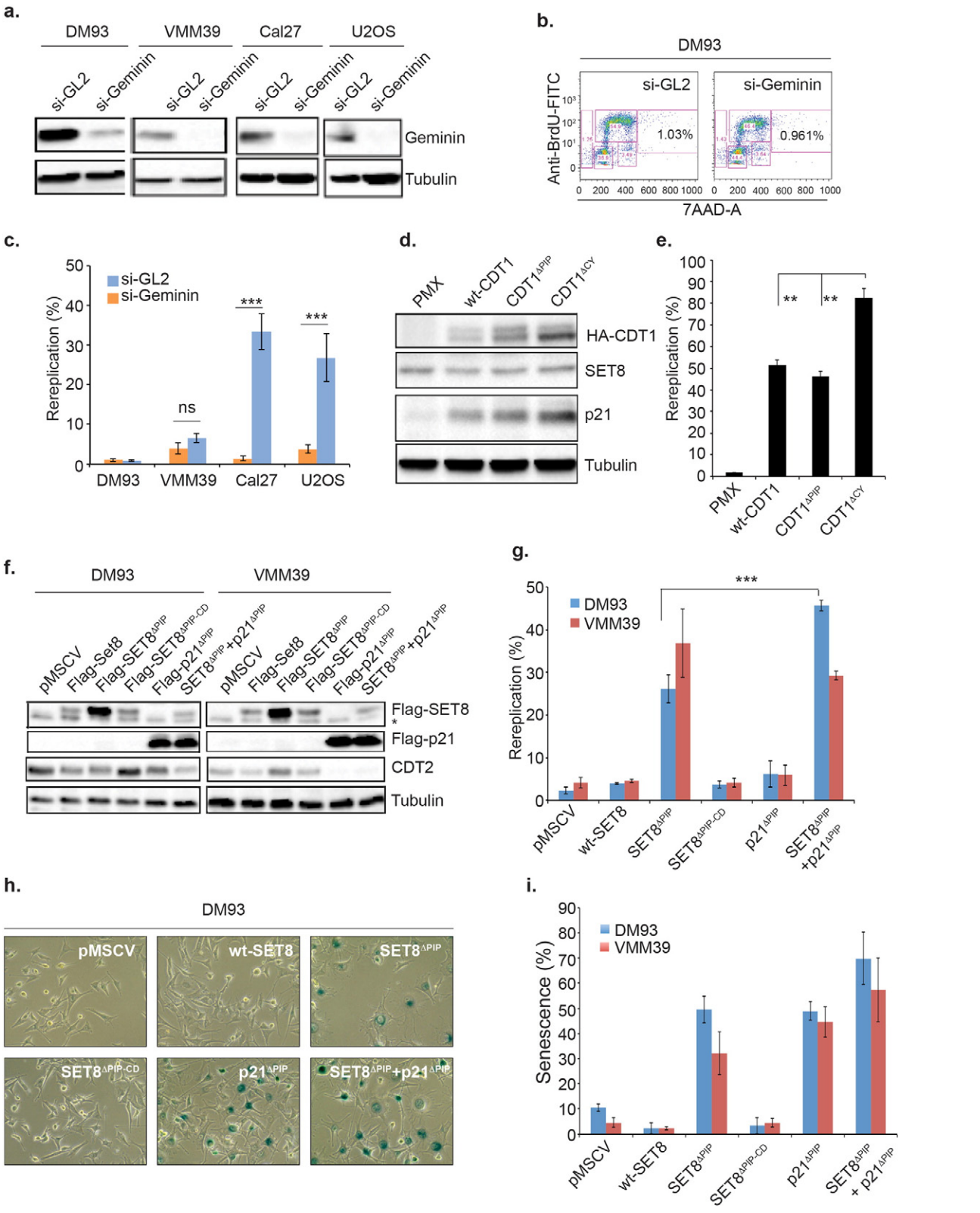


**Fig. 3.** Deregulated stability of catalytically active SET8 and p21 promotes rereplication and senescence in melanoma cells (see also Figure S5). a. Immunoblotting of protein lysates extracted from the indicated cancer cell lines and transfected with si-GL2 or depleted of geminin (si-geminin). Tubulin is a loading control. b. BrdU labeling and FACS analysis of DM93 melanoma cells shown in (a). c. Percentage of cells with rereplication as determined by FACS of the cells shown in (a). Data represent the average of three independent experiments ± S.D. $^{***}p < 0.001$, calculated using Student's *t*-test; ns: non-significant. d. Immunoblotting of control DM39 cells (with empty retrovirus; PMX) or ectopically expressing the indicated CDT1 proteins from retrovirus. e. Percentage of cells with rereplication following transduction with retroviruses expressing the indicated proteins. Data represent the average of three independent experiments ± S.D. $^{**}p < 0.01$, calculated using Student's *t*-test. f. Immunoblotting of DM93 and VMM39 cell extract following transduction with retrovirus expressing the indicated proteins. Tubulin is a loading control. Asterisk: cross-reactive band. g. Percentage of rereplicating DM93 or VMM39 cells treated as in (f) as determined by FACS analysis. Data represent the average of three independent experiments ± S.D. $^{***}p < 0.001$, calculated using Student's *t*-test. h. Representative images of DM93 treated as in (f) and stained with β-gal to monitor senescence. i. Percentage of senescent DM93 and VMM39 cells following the expression of the indicated proteins. Data represent the average of three independent experiments ± S.D.

6 h) increase in CDT1 as well as SET8 protein and activity (H4K20 monomethylation) followed by the appearance of p21 and p27 (Fig. 4b, and Figure S6a and S6b). Increases in CDT1, SET8 and p21 were all attributed to increased stability as well as increase in the stability of not only H4K20me1, but also H4K20me2 and H4K20me3 (Figure S6c–S6f). These latter epigenetic modifications are catalyzed by the SUV4-20H1 and SUV4-20H2 methyltransferase, respectively, and have been shown to be increased in cells with deregulated SET8 stability and contribute to DNA rereplication (Abbas et al., 2010; Beck et al., 2012).

DM93 cells treated with pevonedistat accumulated spontaneous DNA damage (increased γH2AX) and arrested in S and G2/M phases of the cell cycle due to activated DNA damage and G2/M checkpoints *i.e.* increased phosphorylation of CHK1 and CHK2, increased phosphorylation of CDK1 and the accumulation of cells in S and G2 (Fig. 4b, c, and data not shown). This significantly inhibited melanoma cell proliferation (Figure S7b and S7d), concurrently with morphological changes reminiscent to those induced by CDT2 depletion or deletion (Figs. 2b, 4e, 4f and Figure S2e). Consistently, flow cytometry analysis showed 18% of DM93 cells exhibiting >4N DNA content within 24 h, which increased to 68% by 72 h of treatment (Fig. 4c). The extent of rereplication increased with increasing doses of pevonedistat when analyzed at 24 h, and was observed with as low as 500 nM drug concentration (Figure S7a). BrdU labeling illustrated that rereplication occurred within the same cell cycle in 17 and 60% of cells when analyzed at 24 and 48 h, respectively (Figure S7c). While some cells treated with pevonedistat underwent cell death by apoptosis *i.e.* appearance of cleaved PARP protein and increased cells with sub-G1 DNA content (~7%), the majority of cells underwent senescence occurring as early as 48 h post-treatment (Fig. 4b–f).

Using clonogenic survival assays, we found that pevonedistat inhibited the proliferation of DM93 and VMM39, at low drug concentrations of 100 and 50 nM, respectively (Fig. 4d and Figure S4e). Cell viability and proliferation assays demonstrated that pevonedistat effectively inhibited all the melanoma lines tested, with VMM39 and DM13 being the most sensitive with $IC_{50}$ of 35 and 40 nM, respectively (Fig. 4g). VMM1 melanoma cells on the other hand, were least sensitive with an $IC_{50}$ of 330 nM. Pevonedistat resulted in varying degrees of rereplication in these cells (Fig. 4h and Figure S7f). For example, whereas pevonedistat treatment of DM93 cells resulted in 60% of the cells undergoing rereplication at 72 h post-treatment, only 25% of VMM1 and 13.7% of DM13 cells rereplicated their DNA. SLM2 melanoma cells with wt *BRAF*, *NRAS*, *TP53* and *CDKN2A* also exhibited robust rereplication with >58% of cells with rereplication at 72 h post-treatment. Although CDT2 expression in the various lines did not correlate significantly with the IC50 of pevonedistat (Fig. 4g and i), it significantly correlated with pevonedistat-induced rereplication ($r = 0.745$, $p < 0.01$) (Fig. 4j). Strikingly, ectopic overexpression of wt CDT2 in two melanoma cell lines with low expression of CDT2 (VMM1 and DM13) resulted in the induction of statistically significant more rereplication in response to pevonedistat than control cells with empty virus (pMSCV) (Fig. 4k and l). This did not occur with overexpression of a mutant CDT2 protein ($CDT2^{R246A}$), which cannot bind DDB1 and is thus incapable of assembling functioning $CRL4^{CDT2}$ ligase (Jin et al., 2006). This result provides evidence that CDT2 expression directly relates to the efficacy of pevonedistat to induce rereplication *in vitro* through its ubiquitylation activity. Finally, although pevonedistat induced rereplication in all the examined melanoma lines, it induced robust senescence only in cells with wt *CDKN2A* (encoding p16), with minimal impact in cells with an inactivated *CDKN2A* gene (VMM1, DM13 and VMM18 cells), similar to what is observed in si-CDT2 cells (Fig. 2i and 4m). Collectively, these results demonstrate that pevonedistat treatment of melanoma cells is associated with the hallmark of $CRL4^{CDT2}$ inactivation observed with CDT2 depletion or deletion. The results also demonstrate the efficacy of pevonedistat to inhibit melanoma *in vitro*, irrespective of the *BRAF*/*NRAS* or *CDKN2A* mutational status, although the latter may be important for pevonedistat-induced senescence.

### 3.5. Transient Exposure to Pevonedistat Is Sufficient to Induce Rereplication and Permanent Growth Arrest in Melanoma Cells, but Not in Immortalized Non-Transformed Melanocytes

To determine the relationship between the ability of pevonedistat to induce rereplication in melanoma cells and its inhibitory activity, we treated DM93 or VMM39 cells with pevonedistat for 4, 8, 12 or 24 h, washed the drug extensively, and incubated cells with fresh media for various time points. The results demonstrated that cells exposed to pevonedistat for 4 or 8 h were transiently inhibited, but resumed proliferation 24 h later (Fig. 5a–c, and Figure S8a and S8b). This coincided with restoration of cullin neddylation, and the destabilization of CDT1, SET8 and p21 (Fig. 5a). In contrast, cells treated with pevonedistat for 12 or 24 h remained arrested, and exhibited 18% and 60% rereplication, respectively when analyzed 48 h later and were senescent (Fig. 5a–c and data not shown). The reduction in the percentage of rereplicating cells at 48, 72 and 92 h following transient exposure for 12 or 24 h is explained by the continuous proliferation of cells that did not undergo rereplication following drug removal. DM93 cells treated for 12 or 24 h maintained high levels of p21, but not CDT1 or SET8 (Fig. 5a), suggesting that p21 may be essential for maintaining the rereplication phenotype. Furthermore, treatment of DM93 cells with vemurafenib induced robust G1 growth arrest and complete depletion of S-phase cells, and inhibited pevonedistat-induced rereplication (Fig. 5d and e). This result, and the fact that it takes at least 24 h to achieve permanent growth inhibition, demonstrates that pevonedistat-induced rereplication requires that cells remain in active replicative phase, and that a sufficient time of exposure (12–24 h) is necessary to permanently arrest all cycling cells.

Unlike melanoma cells, the treatment of PIG3V or PIG1 immortalized melanocytic cell lines with pevonedistat resulted in only modest inhibition of proliferation with an IC50 of >500 nM (Fig. 4g). Although the continuous treatment of PIG3V with 1 μM pevonedistat inhibited proliferation (Figure S8d and S8e), this was not associated with rereplication or senescence (Figure S7c and S8g). This was not due to a lack of inhibition of $CRL4^{CDT2}$, as these cells accumulated the $CRL4^{CDT2}$ substrates CDT1, p21 and SET8 (which were only transiently upregulated) as well as other cullin substrates, such as p27, with similar kinetics as in DM93 (Fig. 5a and Figure S8c). PIG3V melanocytes exposed to 1 μM pevonedistat for 24 h arrested in G1, but resumed cycling following drug removal, and this was associated with the reversal of cullin neddylation and $CRL4^{Cdt2}$ substrate accumulation, including p21 (Figure S8c–S8f).

### 3.6. Pevonedistat Induces Permanent Growth Inhibition in Melanoma Cells Through SET8- and p21-Dependent Rereplication and Senescence

The lack of significant correlation between pevonedistat-induced rereplication and toxicity prompted us to investigate the contribution of rereplication and/or senescence to pevonedistat-induced toxicity. To achieve this, we first show that siRNA-mediated depletion of CDT1, SET8 or p21 all inhibited pevonedistat-induced rereplication, and senescence (Figure S9), similar to what we observed following CDT2 depletion. Next, we utilized the CRISPR/Cas9 editing tools in an attempt to generate melanoma cells with deletion in *CDKN1A* (encoding p21) or *SET8*. We obtained several clones of DM93 cells, but none had biallelic deletion of either gene (Figure S10). Although we were surprised that none of the clones we obtained were biallelically deleted of *CDKN1A*, the lack of clones with complete deletion of *SET8* is consistent with the important role of SET8 in cell viability (Oda et al., 2010; Schotta et al., 2008). Nevertheless, several clones exhibited a loss of one allele of *CDKN1A* (sg-p21-1-6), and these exhibited significantly reduced levels of p21 in pevonedistat-treated cells (Fig. 5f and Figure S10a–S10c). We also obtained several clones of DM93 cells with monoallelically deleted *SET8* (sg-*SET8*-*1*-*6*), and these had significantly reduced levels of SET8 protein (Fig. 5f and Figure S10d–S10f). The sg-SET8 cells exhibited

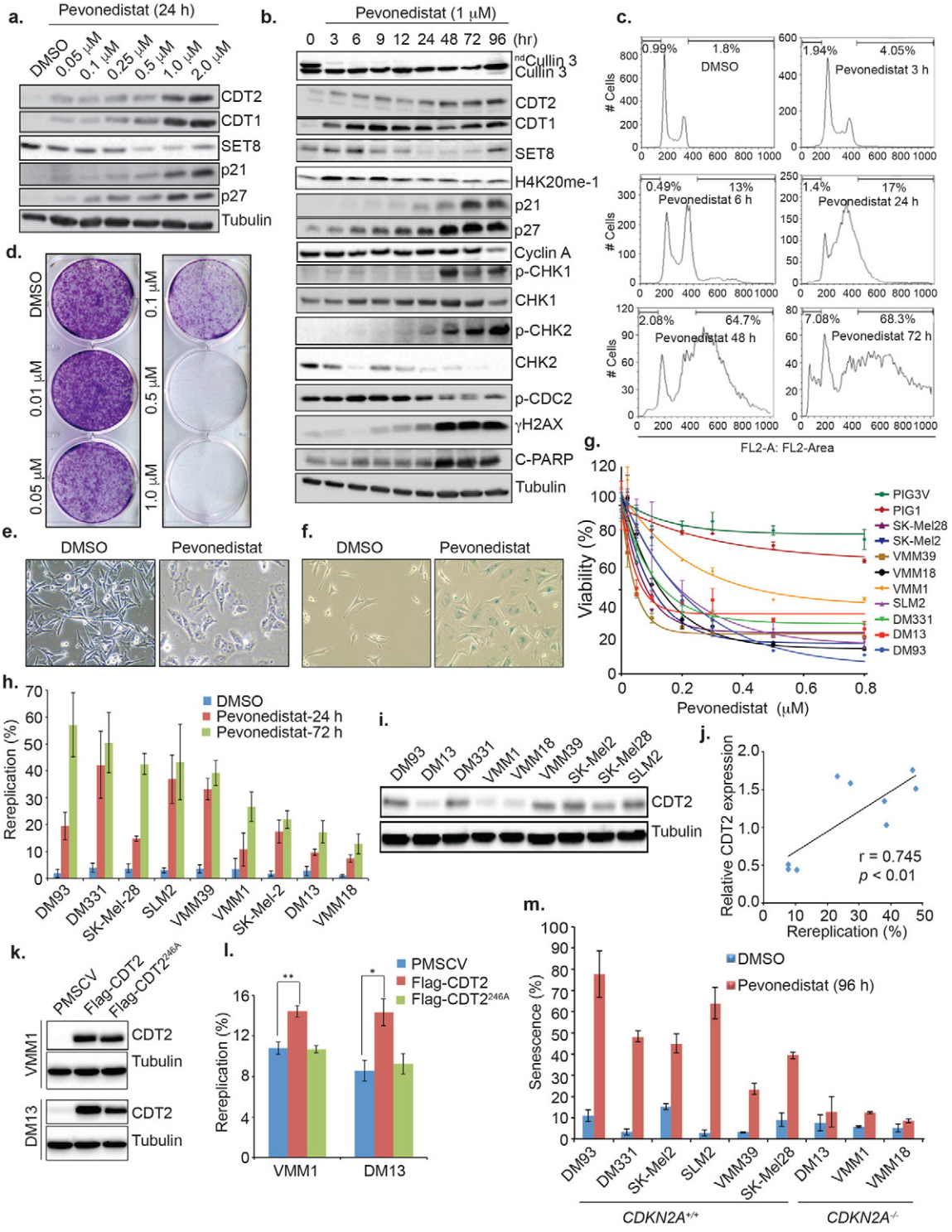


**Fig. 4.** Pevonedistat inhibits melanoma cell proliferation and induces rereplication and senescence, irrespective of the *BRAF* mutational status, and elevated CDT2 expression renders melanoma cells sensitive to pevonedistat-induced rereplication (see also Figures S6 and S7). a. Immunoblotting of cell lysates following treatment with the indicated doses of pevonedistat analyzed 24 h post-treatment. Tubulin is a loading control. b. Same as (a) except cells were treated with 1 μM pevonedistat and cells harvested at the indicated time points following treatment. $^{nd}$Cullin 3: neddylated cullin 3. c. FACS analysis (PI staining) of cells treated with 1 μM pevonedistat for the indicated time points. Percentage of cells with rereplication (>G2/M DNA content) or undergoing apoptosis (sub-G1 DNA content) is also indicated. d. Representative images of clonogenic survival assays of DM93 melanoma cells treated with the indicated doses of pevonedistat. e. Representative phase contrast images of DM93 cells treated with DMSO (solvent) or pevonedistat (1 μM) for 24 h. f. Representative images of DM93 cells treated with pevonedistat for 96 h, and stained with β-gal. g. Viability assays of the indicated melanoma lines and melanocytic PIG1 and PIG3V following treatment with the indicated doses of pevonedistat and expressed as a percentage of control DMSO-treated samples. Data represent the average of three independent experiments ± S.D. h. The percentage of melanoma lines with rereplication following treatment with 1 μM pevonedistat as analyzed by FACS at 24 or 72 h. Data represent the average of three independent experiments ± S.D. i. Steady state CDT2 protein expression in the indicated melanoma cells as determined by immunoblotting. Tubulin is a loading control. j. Correlations between the steady state level of CDT2 protein in various cancer cell lines shown in (i) and the DNA rereplication at 24 h post-treatment shown in (h). k. Immunoblotting of Flag-CDT2 or FLAG-CDT2$^{R246A}$ proteins following their ectopic and stable expression in VMM1 or DM13 melanoma cells from retrovirus. Tubulin is a loading control. l. Percentage of cells in (k) undergoing rereplication following pevonedistat treatment (1 μM) for 72 h, as determined by FACS analysis. Data represent the average of three independent experiments ± S.D. $^{*}p < 0.05$; $^{**}p < 0.01$, calculated using Student's *t*-test. m. Percentage of the indicated melanoma lines undergoing senescence following treatment with 1 μM pevonedistat and analyzed 96 h following treatment. Data represent the average of three independent experiments ± S.D.

normal levels of bulk H4K20me1 and proliferated with similar rates as parental or control DM93 cells (Fig. 5i, and data not shown). Strikingly, both p21 and SET8 hypomorphic DM93 cells were significantly resistant to pevonedistat-induced rereplication and senescence, despite cullin deneddylation, and the upregulation of CDT1 protein (Fig. 5f–h, and Figure S10c and S10f). This result demonstrates that increased endogenous levels of CDT1 is not sufficient to induce rereplication or senescence in the presence of lower levels of SET8 or p21, and further suggests that pevonedistat-induced senescence in melanoma cells is a consequence of DNA rereplication. Given that melanoma cells with higher levels of CDT2 are more susceptible to pevonedistat-induced rereplication (Fig. 4h–l), and only the overexpression of $CRL4^{CDT2}$-resistant, but not $CRL4^{CDT2}$-sensitive form of SET8 is sufficient to trigger rereplication (Fig. 3g), the failure of pevonedistat to induce rereplication and senescence in sg-p21 or sg-SET8 cells highly suggest that pevonedistat-induced rereplication and senescence in melanoma cells is mediated through $CRL4^{CDT2}$ inhibition and the stabilization of SET8 and p21 proteins.

When added continuously in culture, pevonedistat still inhibited the proliferation of sg-p21 and sg-SET8 cells (Fig. 5i). Strikingly however, unlike control cells (sg-control), cells with reduced expression of p21 or SET8 resumed proliferation following the cessation of pevonedistat treatment (Fig. 5i and j). Thus, pevonedistat inhibits the proliferation of melanoma cells through the induction of SET8- and p21-dependent rereplication mechanism, as well as through another mechanism that only transiently inhibits cell proliferation. The result also explains the lack of a significant correlation between pevonedistat-inhibitory activity (IC50) and the induction of rereplication.

### *3.7. Pevonedistat Exerts Anti-Melanoma Activity Through $CRL4^{CDT2}$ Inhibition and Stabilization of SET8 and p21, Irrespective of BRAF/NRAS Mutational Status*

To examine the efficacy of pevonedistat to inhibit melanoma *in vivo*, we inoculated nude mice with DM93 cells and monitored tumor growth. When tumors reached 100–150 $mm^3$ in volume, randomized group of mice (n = 12) were treated with DMSO or with 30 or 60 mg/kg for 5 consecutive days for two cycles separated by 5 days of no treatment (Soucy et al., 2009). Animals were weighted and monitored daily and the drug was well tolerated (Figure S11, and data not shown). Fig. 6a demonstrates that pevonedistat significantly suppressed DM93 melanoma xenografts at 30 mg/kg ($p = 7.7 \times 10^{-3}$) or 60 mg/kg ($p = 2.3 \times 10^{-3}$), but did not result in tumor regression, consistent with the lack of significant apoptotic effect of this drug *in vitro*. Tumor regrowth was not detectable at either drug concentration as monitored up to 10 days following the cessation of treatment. Analysis of tumor extracts of treated animals (on day 25) demonstrates that pevonedistat inhibited cullin neddylation and resulted in the accumulation of cullin substrates (CDT2, CDT1, and p21) and spontaneous DNA damage, and exhibited activated checkpoints (Fig. 6b). Because SET8 protein is only transiently increased by pevonedistat, we did not detect significant increases of SET8 in these tumor lysates at this late time point. Importantly, although pevonedistat (30 mg/kg) significantly inhibited the growth of sg-control DM93 xenografts ($p = 0.009$), it failed to inhibit the growth of sg-p21-1 or sg-SET8-1 DM93 xenografts ($p = 0.092$ and 0.66, respectively) (Fig. 6c). This result provides evidence that targeted inactivation of the $CRL4^{CDT2}$ E3 ligase, and the stabilization of its substrates p21 and SET8, is the primary mechanism underlying the anti-melanoma activity of pevonedistat *in vivo*.

To test whether pevonedistat also inhibits non-BRAF melanomas, we established xenografts of VMM39 (with *NRAS* and *PDGFR* activating mutations) or SLM2 cells (without *NRAS* or *BRAF* mutations). Fig. 7a and b demonstrate that the administration of pevonedistat (60 mg/kg) significantly inhibited the growth of VMM39 and SLM2 xenografts ($p = 1.8 \times 10^{-5}$, and $2.3 \times 10^{-3}$, respectively), although tumor regrowth was apparent in these xenografts following the cessation of drug administration. Similar to DM93 xenografts, pevonedistat inhibited the deneddylation of cullins and induced the accumulation of CDT1 and p21 proteins in the VMM39 xenografts, even when tumors were analyzed 10 days following the cessation of treatment (Figure S11b). Pevonedistat also inhibited, albeit to a lesser extent, the growth of DM331 xenografts, a mutant BRAF melanoma cell line resistant to the BRAF kinase inhibitors vemurafenib or PLX4720, a structural analogue and precursor of vemurafenib with more potent activity in rodents (Tsai et al., 2008) (Fig. 7c and Figure S12; and (Roller et al., 2015)). Although these xenografts were nevertheless inhibited by PLX4720, the combined administration of pevonedistat and PLX4720 resulted in synergistic inhibition (Fig. 7c). Finally, DM331 cells, as well as the BRAF-mutant SK-MEL-24 cells, extracted *ex-vivo* from PLX4720-resistant tumors (Roller et al., 2015), remained insensitive to vemurafenib, but were sensitive to pevonedistat-induced rereplication and inhibition *in vitro* (Fig. 7d–g). Collectively, these results demonstrate that the administration of pevonedistat as a single agent inhibits melanoma *in vivo*, irrespective of the *BRAF*/*NRAS* mutational status, synergizes with PPLX4720 to inhibit BRAF melanoma proliferation, and effectively inhibits PLX4720-relapsed melanoma cell growth.

## 4. Discussion

We identified the $CRL4^{CDT2}$ E3 ubiquitin ligase as a molecular therapeutic target in melanoma. CDT2 knockdown or the pharmacological inhibition of $CRL4^{CDT2}$ activity by the neddylation inhibitor pevonedistat inhibits melanoma cell proliferation *in vitro* and *in vivo* through the induction of SET8- and p21-dependent aberrant DNA replication and the induction of p21-dependent cellular senescence. This occurs irrespective of the *BRAF* or *NRAS* mutational status. Although p16 may also be involved in rereplication-induced senescence, it is not essential for pevonedistat-induced toxicity, and thus, mutational inactivation of the *CDKN2A* or oncogenic activation of *BRAF* or *NRAS*, all common genetic defects in melanoma, do not present an obstacle for the therapeutic efficacy of pevonedistat. Pevonedistat was also efficacious in suppressing melanoma cells that are resistant to vemurafenib treatment *in vitro* and synergized with PLX4720 to suppress mutant *BRAF* melanoma. It remains to be determined however, whether $CRL4^{CDT2}$ inhibition, or the stabilization of SET8 or p21, contributes to the synergistic activity of pevonedistat with PLX4720. Nevertheless, our findings suggest that pevonedistat may be most efficacious if administered along with other melanoma inhibitors, such as vemurafenib (for BRAF melanomas), and may also be considered as a second line therapeutic for vemurafenib- or other BRAF kinase inhibitor-relapsed melanoma patients.

Mechanistically, we show that $CRL4^{CDT2}$ is the primary target of inactivation by pevonedistat in melanoma and that its toxicity is dependent primarily on the stabilization of the $CRL4^{CDT2}$ substrates SET8 and p21 both *in vitro* and *in vivo*. The lack of a therapeutic response on melanoma cells with hypomorphic expression of SET8 or p21 provides solid genetic evidence that the main anti-melanoma activity of pevonedistat is associated with the drug's ability to promote rereplication and permanent growth inhibition through preventing SET8 and p21 proteolytic degradation. Pevonedistat however, also transiently inhibits melanoma proliferation through an unknown mechanism. We speculate that this may be dependent on the accumulation of other cullin substrates and may include the CDK2 inhibitor p27, an $SCF^{SKP2}$ ubiquitylation substrate, which is also stabilized by pevonedistat (Fig. 4a and b). This however, is insufficient to halt melanoma proliferation in the absence of SET8- and p21-mediated cytotoxicities (Fig. 6c).

Whereas the $CRL4^{CDT2}$ substrates CDT1 and p21 are independently required to induce rereplication and senescence in melanoma cells with inactivated $CRL4^{CDT2}$, SET8 is both necessary and sufficient to promote rereplication and the ensuing senescence. The exact mechanism by which increased SET8 protein stability promotes rereplication is currently unclear, but histone H4K20 methylation may be critical for this activity (Abbas et al., 2010; Tardat et al., 2010). The main role of p21 on the other hand, appears to halt cell cycle progression (thus

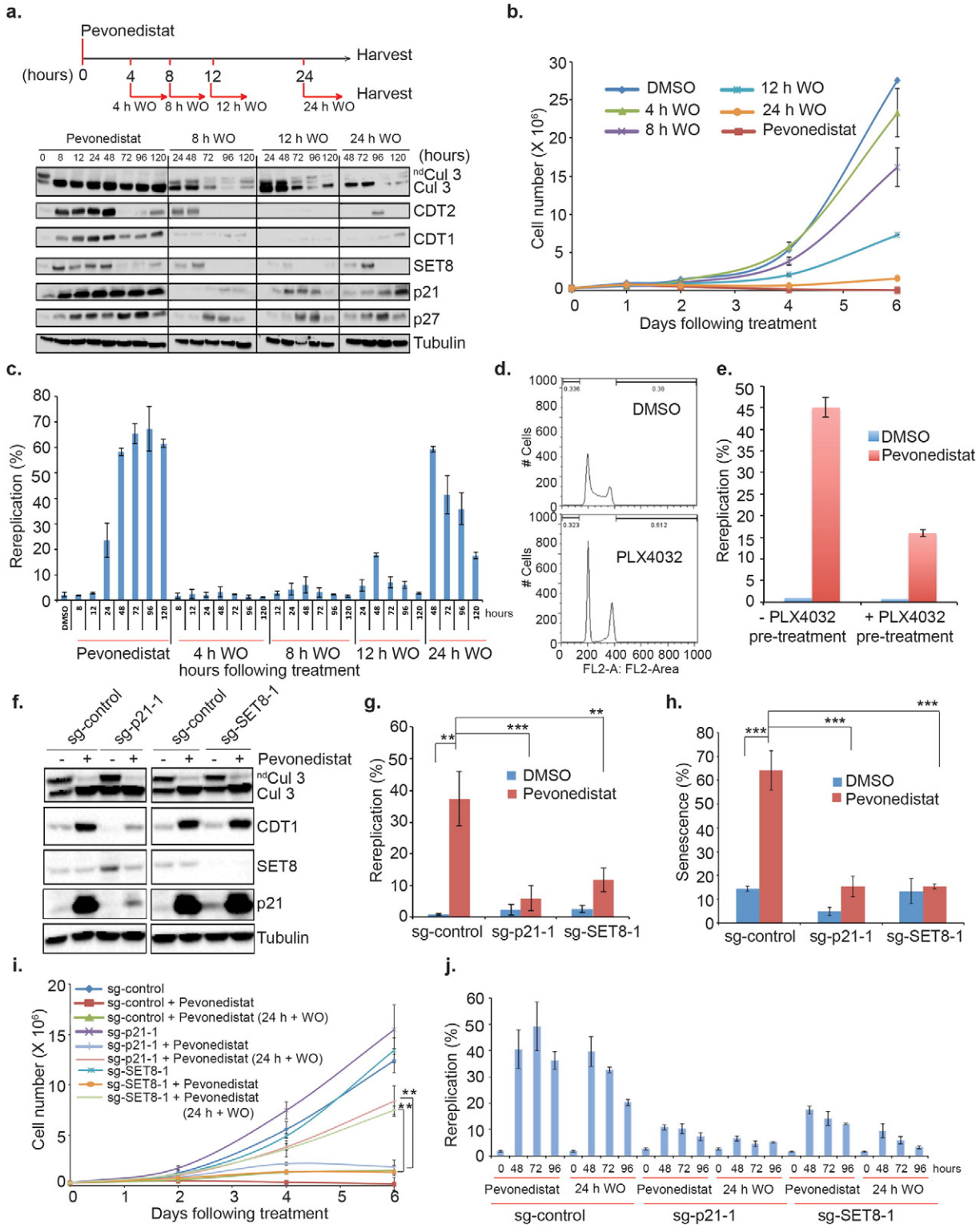


**Fig. 5.** Transient exposure of melanoma cells to pevonedistat induces p21- and SET8-dependent permanent growth inhibition and senescence (see also Figure S10). a. Immunoblotting of protein extracts of DM93 cells treated with 1 μM pevonedistat and harvested according the schematic time line of drug addition and withdrawal (wash out (WO); Top). Tubulin is loading control. $^{nd}$Cul3: neddylated Cullin 3. b. Proliferation of DM93 cells treated according to the schematic in (a) as determined by cell counting. Data represent the average of three independent experiments ± S.D. c. Percentage of DM93 cells shown in (a) undergoing rereplication as determined by PI staining and FACS analysis. Data represent the average of three independent experiments ± S.D. d. FACS analysis (PI staining) of DM93 cells treated with vemurafenib (PLX4032) for 24 h showing the induction of G1 cell cycle arrest. e. Percentage of DM93 cells undergoing rereplication with or without vemurafenib treatment for 24 h before the addition of pevonedistat for another 48 h. Data represent the average of three independent experiments ± S.D. f. Immunoblotting of protein lysates of individual clones of DM93 cells with hypomorphic expression of p21 (sg-p21-1) or SET8 protein (sg-SET8-1) and treated with 1 μM pevonedistat for 48 h. g–h. Percentage of cells undergoing rereplication (g) and senescence (h) in the cells shown in (f). Data represent the average of three independent experiments ± S.D. *p*-values were calculated using Student's *t*-test. $^{*}p < 0.05$; $^{**}p < 0.01$; $^{***}p < 0.001$. i. Same as in (b), but with the sg-control-1, sg-p21-1 and sg-SET8-1 DM93 cells shown in (f). j. Same as in (c), but with the sg-control-1, sg-p21-1 and sg-SET8-1 DM93 cells shown in (f).

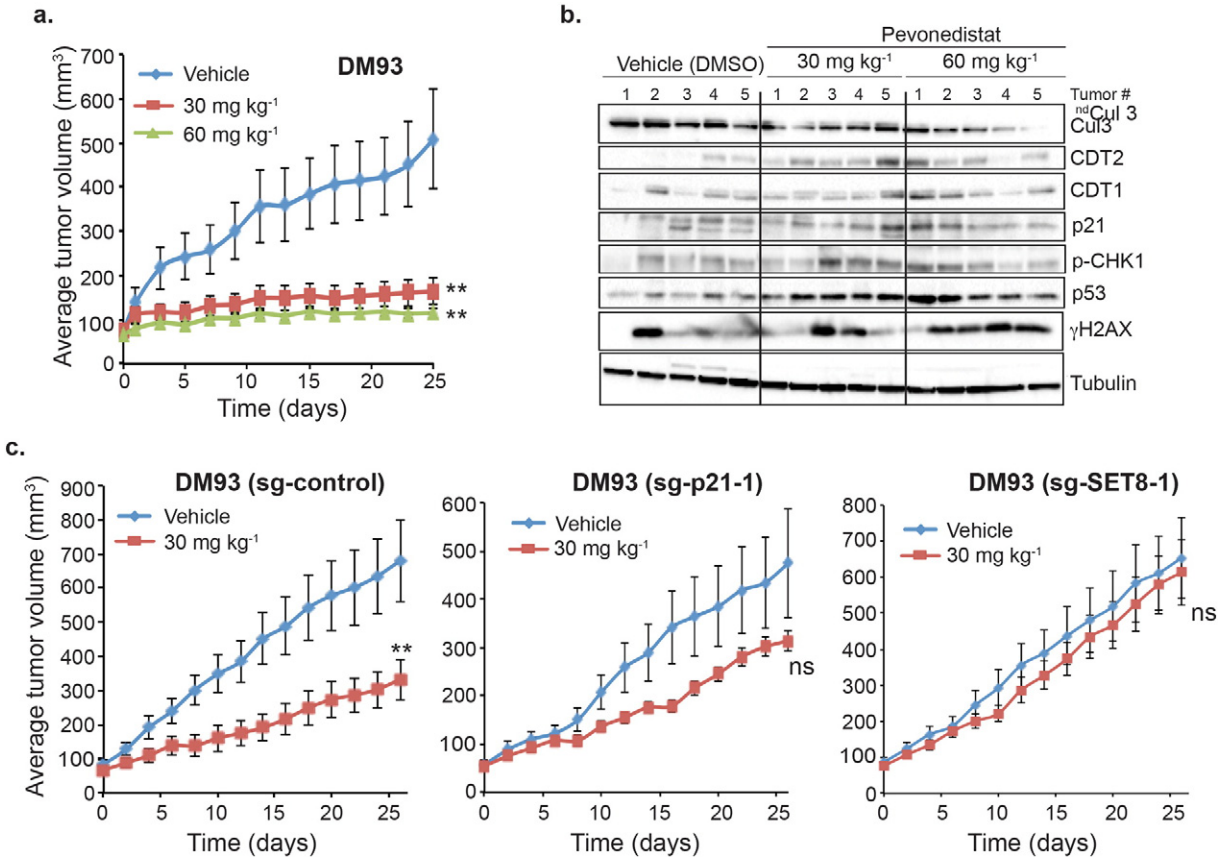


**Fig. 6.** Pevonedistat inhibits melanoma xenografts through p21- and SET8-dependent mechanism (see also Figure S11). a. Nude mice bearing DM93 tumor xenografts were dosed by IP administration with either vehicle (DMSO) or with the indicated doses of pevonedistat according the schedules indicated in Materials & Methods. Mean tumor volumes ± s.e.m. are shown. $n = 12$ mice per group. $p$-values were calculated using Student's $t$-test; $^{**}p < 0.01$. b. Immunoblotting of protein lysates of DM93 tumor xenografts from 5 randomly selected animals of each group (a, extracted on day 25) for the indicated proteins. Tubulin is a loading control. c. Same as in (a), except control DM93 (left; sg-control), or DM93 hypomorphic clones of p21 (sg-p21-1; middle) or SET8 (sg-SET8-1; right) were used to establish the tumor xenografts, and animals were administered pevonedistat (30 mg/kg). Mean tumor volumes ± s.e.m. are shown. $n = 12$ mice per group. $p$-values were calculated using Student's $t$-test; $^{**}p < 0.01$; ns: non-significant ($p > 0.05$).

permitting rereplication) and induce senescence. This is supported by the finding that p21 is critical for the induction of rereplication and senescence in response to $CRL4^{CDT2}$ inactivation (by si-CDT2 or pevonedistat), and is also upregulated in rereplicating cells following the ectopic expression of CDT1 or $SET8^{\Delta PIP}$, or following EMI1 depletion, but is insufficient to induce rereplication.

Although CDT1 promotes rereplication in cancer cells as demonstrated by the robust induction of rereplication through geminin depletion, we did not observe such a role in melanoma cells, likely because CDT1 activity is restrained by cyclin A-dependent $SCF^{SKP2}$ activity. Non-physiological overexpression of CDT1 however, was sufficient to induce rereplication in melanoma cells, but this is likely to also require SET8 and p21. This conclusion is supported by the fact that although pevonedistat induced significant rereplication in melanoma cells, it failed to do so in cells with hypomorphic expression of SET8 or p21, despite significant increases in CDT1 protein. The anti-melanoma activity of pevonedistat and its dependence on $CRL4^{CDT2}$ inhibition and the induction of SET8- and p21-dependent rereplication provide a stronger link between presumed drug target (NAE) and biology than is available for many other "targeted therapies".

Our study also demonstrates that CDT2 is significantly overexpressed in melanoma, and its elevated expression correlates significantly with poor overall and disease-free patient survival. Because elevated CDT2 expression correlates with, and renders melanoma cells more susceptible to, pevonedistat-induced rereplication *in vitro*, and given that rereplication appears to play a major role in mediating its efficacy *in vivo*, we speculate that pevonedistat would be most efficacious in tumors with elevated CDT2 expression. This includes not only melanoma, but also potentially other malignancies with elevated CDT2 expression (Figure S1).

CDT2 is not likely to function as a classical oncogene, but may act as a cancer-associated gene to which cancer cells become "addicted". This is supported by the finding that while $CRL4^{CDT2}$ inactivation by pevonedistat induces rereplication in melanoma cells, it failed to do so in non-cancer melanocytic cells. Similarly, CDT2 depletion in non-cancer cells failed to induce rereplication in non-cancer cells, but did so following the ectopic expression of KRAS (Olivero et al., 2014). We propose that CDT2 is overexpressed in melanoma cells to alleviate replication stress that may be induced by melanoma oncogenes.

Because only transient exposure of melanoma cells to pevonedistat is sufficient to irreversibly arrest melanoma cells with the majority of cells undergoing senescence, and this occurs only in malignant melanoma cells, targeting the $CRL4^{CDT2}$ ubiquitin ligase is an especially attractive therapeutic approach that is likely to be associated with only minimal impact on normal cellular activity or cytotoxicity. Why non-malignant melanocytes exposed to pevonedistat are only transiently inhibited, and without undergoing robust rereplication, is not clear, but our results support the hypothesis that non-cancer cells have additional mechanisms to guard against aberrant DNA rereplication (Abbas et al., 2013).

In summary, our findings illustrate that the $CRL4^{CDT2}$-SET8/p21 degradation axis is a promising new target for inactivation in melanoma. We provide significant evidence for the utility of pevonedistat as an effective single-agent therapeutic for *BRAF* and non-*BRAF* cutaneous

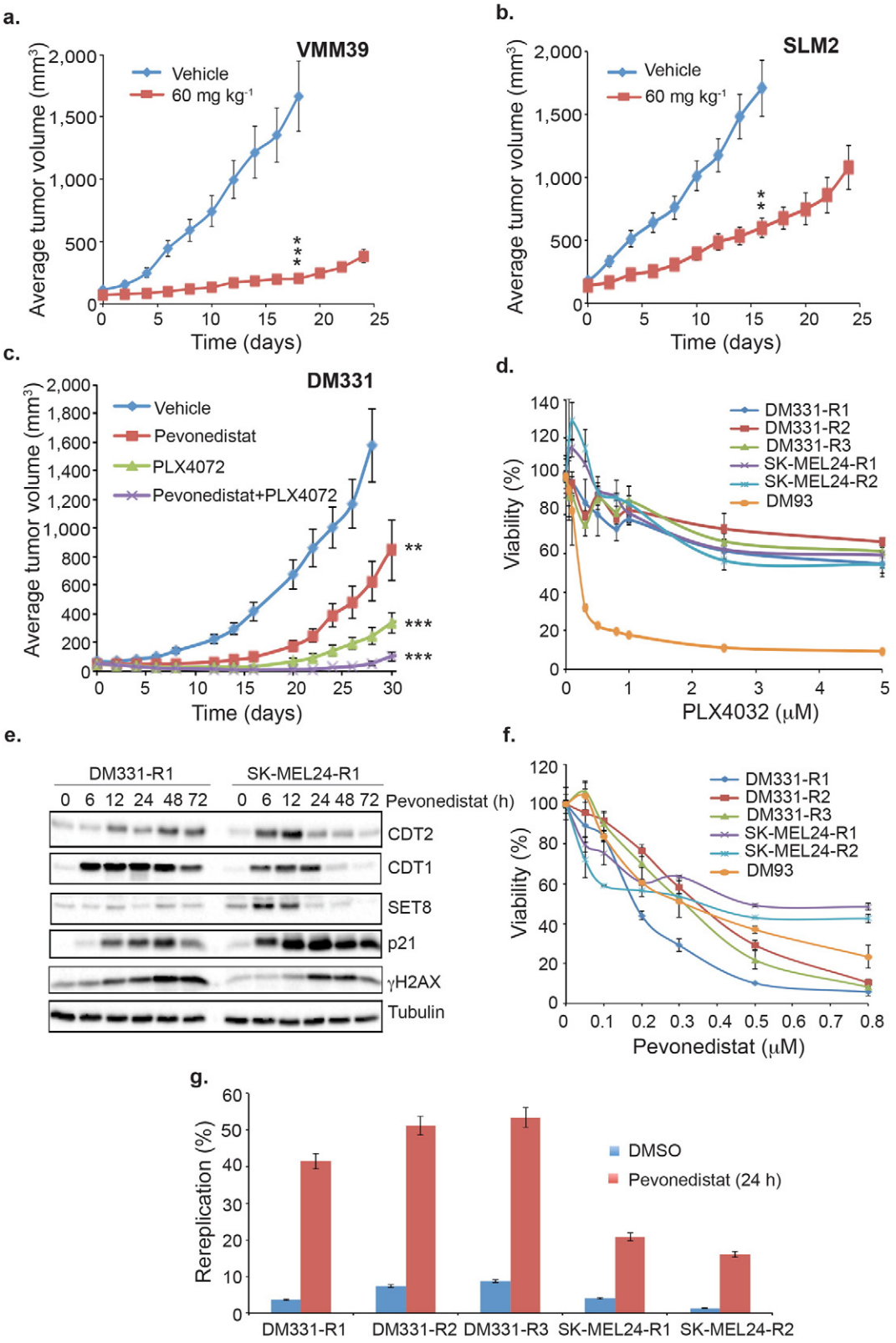


**Fig. 7.** Pevonedistat inhibits melanoma xenografts irrespective of the *BRAF* mutational status and synergizes with the BRAF inhibitor PLX4720 to suppress BRAF melanoma. a-c. Nude mice bearing VMM39 (mut-*NRAS*; a), SLM2 (wt *NRAS*/*BRAF*; b) or DM331 (mut-*BRAF*; c) tumor xenografts were dosed by IP administration (60 mg/kg) pevonedistat according the schedules indicated in Materials & Methods. Mice with DM331 xenograft were also treated with PLX4720, or with pevonedistat and PLX4720 as described in Materials & Methods. Mean tumor volumes ± s.e.m. are shown. $n = 12$ mice per group. *p*-values were calculated using Student's *t*-test; $^{**}p < 0.01$; $^{***}p < 0.001$. d. Viability assays of DM331 (R1-R3) or SK-MEL-24 (R1 and R2) cells extracted *ex vivo* from PLX4720-resistant tumors and treated with the indicated doses of vemurafenib. DM93 cells were similarly analyzed and shown for comparison. The results are expressed as a percentage of control DMSO-treated samples. Data represent the average of three independent experiments ± S.D. e. Immunoblotting of DM331 (R1) and SK-MEL24 (R1) cell extracts following treatment with 1 μM pevonedistat for the indicated time *in vitro*. Tubulin is a loading control. f. Viability assays of DM331 (R1-R3) or SK-MEL-24 (R1 and R2) cells treated with the indicated doses pevonedistat *in vitro*. The results are expressed as a percentage of control DMSO-treated samples. Data represent the average of three independent experiments ± S.D. g. Percentage of DM331 (R1-*R3*) and SK-MEL-24 (R1 and R2) undergoing rereplication following treatment with 1 μM pevonedistat for 72 h. Data represent the average of three independent experiments ± S.D.

melanoma, as a synergistic agent with BRAF kinase inhibitors for BRAF melanoma, and potentially as a second line therapeutic for recurrent melanoma following BRAF-kinase inhibitor monotherapy.

## Conflict of Interest Statement

We declare no financial or other relationship causing conflict of interest in this study.

## Author Contributions

M.B. performed most of the experiments, and analyzed data. F.G. and M.B. performed the animal experiments. K.D. carried out gene knockout experiments and analyzed the results. P.C. aided in the washout experiments. J.O. performed *BRAF* mutational analysis in the TMA. D.G. and C.L.S. contributed to the study design and data analysis. T.A. conceived and designed the study, performed experiments, analyzed data, supervised the overall study, and wrote the manuscript. All authors participated in revising the manuscript.

## Acknowledgments

This work was supported by National Cancer Institute (NCI) grant R00CA140774 to T.A. We thank Patcharin Pramoonjago, Joanne Lannigan for technical assistance with Immunohistochemistry and flow cytometry, respectively. We also thank Donna Deacon for help with the TMAs, and members of the Abbas laboratory for helpful discussions. We also thank Yongjuan Xia at the UNC Translational Pathology Laboratory (TPL) for technical assistance with BRAF-mutational analysis in TMA. We are grateful to Michael J. Weber, David Brautigan and James Larner for critical comments on the manuscript. The authors have filed two patent applications related to this work.

## Appendix A. Supplementary data

Supplementary data to this article can be found online at http://dx.doi.org/10.1016/j.ebiom.2016.06.023.

## References

Abbas, T., Dutta, A., 2011. CRL4Cdt2: master coordinator of cell cycle progression and genome stability. Cell Cycle 10, 241–249.
Abbas, T., Keaton, M.A., Dutta, A., 2013. Genomic instability in cancer. Cold Spring Harb. Perspect. Biol. 5, a012914.
Abbas, T., Shibata, E., Park, J., Jha, S., Karnani, N., Dutta, A., 2010. CRL4(Cdt2) regulates cell proliferation and histone gene expression by targeting PR-Set7/Set8 for degradation. Mol. Cell 40, 9–21.
Abbas, T., Sivaprasad, U., Terai, K., Amador, V., Pagano, M., Dutta, A., 2008. PCNA-dependent regulation of p21 ubiquitylation and degradation via the CRL4Cdt2 ubiquitin ligase complex. Genes Dev. 22, 2496–2506.
Balch, C.M., Gershenwald, J.E., Soong, S.J., Thompson, J.F., Atkins, M.B., Byrd, D.R., Buzaid, A.C., Cochran, A.J., Coit, D.G., Ding, S., et al., 2009. Final version of 2009 AJCC melanoma staging and classification. J. Clin. Oncol. Off. J. Am. Soc. Clin. Oncol. 27, 6199–6206.
Beck, D.B., Burton, A., Oda, H., Ziegler-Birling, C., Torres-Padilla, M.E., Reinberg, D., 2012. The role of PR-Set7 in replication licensing depends on Suv4-20h. Genes Dev. 26, 2580–2589.
Bliss, C., 1939. The toxicity of poisons applied jointly. Ann. Appl. Biol. 585–615.
Cerami, E., Gao, J., Dogrusoz, U., Gross, B.E., Sumer, S.O., Aksoy, B.A., Jacobsen, A., Byrne, C.J., Heuer, M.L., Larsson, E., et al., 2012. The cBio cancer genomics portal: an open platform for exploring multidimensional cancer genomics data. Cancer Discov. 2, 401–404.
Chapman, P.B., Hauschild, A., Robert, C., Haanen, J.B., Ascierto, P., Larkin, J., Dummer, R., Garbe, C., Testori, A., Maio, M., et al., 2011. Improved survival with vemurafenib in melanoma with BRAF V600E mutation. N. Engl. J. Med. 364, 2507–2516.
Collisson, E.A., C., J., Brooks, A.N., Berger, A.H., Lee, W., Chmielecki, J., et al., 2014. Comprehensive molecular profiling of lung adenocarcinoma. Nature 511, 543–550.
Davies, H., Bignell, G.R., Cox, C., Stephens, P., Edkins, S., Clegg, S., Teague, J., Woffendin, H., Garnett, M.J., Bottomley, W., et al., 2002. Mutations of the BRAF gene in human cancer. Nature 417, 949–954.
Davies, M.A., Samuels, Y., 2010. Analysis of the genome to personalize therapy for melanoma. Oncogene 29, 5545–5555.
Erdag, G., Schaefer, J.T., Smolkin, M.E., Deacon, D.H., Shea, S.M., Dengel, L.T., Patterson, J.W., Slingluff Jr., C.L., 2012. Immunotype and immunohistologic characteristics of tumor-infiltrating immune cells are associated with clinical outcome in metastatic melanoma. Cancer Res. 72, 1070–1080.
Fitzgerald, J.B., Schoeberl, B., Nielsen, U.B., Sorger, P.K., 2006. Systems biology and combination therapy in the quest for clinical efficacy. Nat. Chem. Biol. 2, 458–466.
Flaherty, K.T., Puzanov, I., Kim, K.B., Ribas, A., McArthur, G.A., Sosman, J.A., O'Dwyer, P.J., Lee, R.J., Grippo, J.F., Nolop, K., et al., 2010. Inhibition of mutated, activated BRAF in metastatic melanoma. N. Engl. J. Med. 363, 809–819.
Gao, J., Aksoy, B.A., Dogrusoz, U., Dresdner, G., Gross, B., Sumer, S.O., Sun, Y., Jacobsen, A., Sinha, R., Larsson, E., et al., 2013. Integrative analysis of complex cancer genomics and clinical profiles using the cBioPortal. Sci. Signal. 6, pl1.
Garcia, K., Blank, J.L., Bouck, D.C., Liu, X.J., Sappal, D.S., Hather, G., Cosmopoulos, K., Thomas, M.P., Kuranda, M., Pickard, M.D., et al., 2014. Nedd8-activating enzyme inhibitor MLN4924 provides synergy with mitomycin C through interactions with ATR, BRCA1/BRCA2, and chromatin dynamics pathways. Mol. Cancer Ther. 13, 1625–1635.
Glickman, M.H., Ciechanover, A., 2002. The ubiquitin-proteasome proteolytic pathway: destruction for the sake of construction. Physiol. Rev. 82, 373–428.
Godbersen, J.C., Humphries, L.A., Danilova, O.V., Kebbekus, P.E., Brown, J.R., Eastman, A., Danilov, A.V., 2014. The Nedd8-activating enzyme inhibitor MLN4924 thwarts microenvironment-driven NF-kappaB activation and induces apoptosis in chronic lymphocytic leukemia B cells. Clin. Cancer Res. 20, 1576–1589.
Gu, Y., Kaufman, J.L., Bernal, L., Torre, C., Matulis, S.M., Harvey, R.D., Chen, J., Sun, S.Y., Boise, L.H., Lonial, S., 2014. MLN4924, an NAE inhibitor, suppresses AKT and mTOR signaling via upregulation of REDD1 in human myeloma cells. Blood 123, 3269–3276.
Hersey, P., Bastholt, L., Chiarion-Sileni, V., Cinat, G., Dummer, R., Eggermont, A.M., Espinosa, E., Hauschild, A., Quirt, I., Robert, C., et al., 2009. Small molecules and targeted therapies in distant metastatic disease. Annals Oncol. 20 (Suppl. 6), vi35-40.
Hogan, K.T., Sutton, J.N., Chu, K.U., Busby, J.A., Shabanowitz, J., Hunt, D.F., Slingluff Jr., C.L., 2005. Use of selected reaction monitoring mass spectrometry for the detection of specific MHC class I peptide antigens on A3 supertype family members. Cancer Immunol. Immunother. 54, 359–371.
Huntington, J.T., Shields, J.M., Der, C.J., Wyatt, C.A., Benbow, U., Slingluff Jr., C.L., Brinckerhoff, C.E., 2004. Overexpression of collagenase 1 (MMP-1) is mediated by the ERK pathway in invasive melanoma cells: role of BRAF mutation and fibroblast growth factor signaling. J. Biol. Chem. 279, 33168–33176.
Jackson, S., Xiong, Y., 2009. CRL4s: the CUL4-RING E3 ubiquitin ligases. Trends Biochem. Sci. 34, 562–570.
Jazaeri, A.A., Shibata, E., Park, J., Bryant, J.L., Conaway, M.R., Modesitt, S.C., Smith, P.G., Milhollen, M.A., Berger, A.J., Dutta, A., 2013. Overcoming platinum resistance in preclinical models of ovarian cancer using the neddylation inhibitor MLN4924. Mol. Cancer Ther. 12, 1958–1967.
Jin, J., Arias, E.E., Chen, J., Harper, J.W., Walter, J.C., 2006. A family of diverse Cul4-Ddb1-interacting proteins includes Cdt2, which is required for S phase destruction of the replication factor Cdt1. Mol. Cell 23, 709–721.
Kittlesen, D.J., Thompson, L.W., Gulden, P.H., Skipper, J.C., Colella, T.A., Shabanowitz, J., Hunt, D.F., Engelhard, V.H., Slingluff Jr., C.L., 1998. Human melanoma patients recognize an HLA-A1-restricted CTL epitope from tyrosinase containing two cysteine residues: implications for tumor vaccine development. J. Immunol. 160, 2099–2106.
Le Poole, I.C., Boissy, R.E., Sarangarajan, R., Chen, J., Forristal, J.J., Sheth, P., Westerhof, W., Babcock, G., Das, P.K., Saelinger, C.B., 2000. PIG3V, an immortalized human vitiligo melanocyte cell line, expresses dilated endoplasmic reticulum. In Vitro Cell. Dev. Biol. Anim. 36, 309–319.
Li, H., Tan, M., Jia, L., Wei, D., Zhao, Y., Chen, G., Xu, J., Zhao, L., Thomas, D., Beer, D.G., et al., 2014a. Inactivation of SAG/RBX2 E3 ubiquitin ligase suppresses KrasG12D-driven lung tumorigenesis. J. Clin. Invest. 124, 835–846.
Li, L., Wang, M., Yu, G., Chen, P., Li, H., Wei, D., Zhu, J., Xie, L., Jia, H., Shi, J., et al., 2014b. Overactivated neddylation pathway as a therapeutic target in lung cancer. J. Natl. Cancer Inst. 106.
Lin, J.J., Milhollen, M.A., Smith, P.G., Narayanan, U., Dutta, A., 2010. NEDD8-targeting drug MLN4924 elicits DNA rereplication by stabilizing Cdt1 in S phase, triggering checkpoint activation, apoptosis, and senescence in cancer cells. Cancer Res. 70, 10310–10320.
Lovly, C.M., Shaw, A.T., 2014. Molecular pathways: resistance to kinase inhibitors and implications for therapeutic strategies. Clin. Cancer Res. 20, 2249–2256.
Luo, J., Solimini, N.L., Elledge, S.J., 2009. Principles of cancer therapy: oncogene and non-oncogene addiction. Cell 136, 823–837.
Machida, Y.J., Dutta, A., 2007. The APC/C inhibitor, Emi1, is essential for prevention of rereplication. Genes Dev. 21, 184–194.
Merlet, J., Burger, J., Gomes, J.E., Pintard, L., 2009. Regulation of cullin-RING E3 ubiquitin-ligases by neddylation and dimerization. Cell. Mol. Life Sci. 66, 1924–1938.
Milhollen, M.A., Narayanan, U., Soucy, T.A., Veiby, P.O., Smith, P.G., Amidon, B., 2011. Inhibition of NEDD8-activating enzyme induces rereplication and apoptosis in human tumor cells consistent with deregulating CDT1 turnover. Cancer Res. 71, 3042–3051.
Milhollen, M.A., Traore, T., Adams-Duffy, J., Thomas, M.P., Berger, A.J., Dang, L., Dick, L.R., Garnsey, J.J., Koenig, E., Langston, S.P., et al., 2010. MLN4924, a NEDD8-activating enzyme inhibitor, is active in diffuse large B-cell lymphoma models: rationale for treatment of NF-{kappa}B-dependent lymphoma. Blood 116, 1515–1523.
Molhoek, K.R., Griesemann, H., Shu, J., Gershenwald, J.E., Brautigan, D.L., Slingluff Jr., C.L., 2008. Human melanoma cytolysis by combined inhibition of mammalian target of rapamycin and vascular endothelial growth factor/vascular endothelial growth factor receptor-2. Cancer Res. 68, 4392–4397.
Nakagawa, H., Tategu, M., Yamauchi, R., Sasaki, K., Sekimachi, S., Yoshida, K., 2008. Transcriptional regulation of an evolutionary conserved intergenic region of CDT2-INTS7. PLoS One 3, e1484.

Oda, H., Hubner, M.R., Beck, D.B., Vermeulen, M., Hurwitz, J., Spector, D.L., Reinberg, D., 2010. Regulation of the histone H4 monomethylase PR-Set7 by CRL4(Cdt2)-mediated PCNA-dependent degradation during DNA damage. Mol. Cell 40, 364–376.

Olivero, M., Dettori, D., Arena, S., Zecchin, D., Lantelme, E., Di Renzo, M.F., 2014. The stress phenotype makes cancer cells addicted to CDT2, a substrate receptor of the CRL4 ubiquitin ligase. Oncotarget 5, 5992–6002.

Roller, D.G., Capaldo, B., Bekiranov, S., Mackey, A.J., Conaway, M.R., Petricoin, E.F., Gioeli, D., Weber, M.J., 2015. Combinatorial drug screening and molecular profiling reveal diverse mechanisms of intrinsic and adaptive resistance to BRAF inhibition in V600E BRAF mutant melanomas. Oncotarget.

Schotta, G., Sengupta, R., Kubicek, S., Malin, S., Kauer, M., Callen, E., Celeste, A., Pagani, M., Opravil, S., De La Rosa-Velazquez, I.A., et al., 2008. A chromatin-wide transition to H4K20 monomethylation impairs genome integrity and programmed DNA rearrangements in the mouse. Genes Dev. 22, 2048–2061.

Senga, T., Sivaprasad, U., Zhu, W., Park, J.H., Arias, E.E., Walter, J.C., Dutta, A., 2006. PCNA is a cofactor for Cdt1 degradation by CUL4/DDB1-mediated N-terminal ubiquitination. J. Biol. Chem. 281, 6246–6252.

Siegel, R., DeSantis, C., Virgo, K., Stein, K., Mariotto, A., Smith, T., Cooper, D., Gansler, T., Lerro, C., Fedewa, S., et al., 2012. Cancer treatment and survivorship statistics, 2012. CA Cancer J. Clin. 62, 220–241.

Slingluff Jr., C.L., Cox, A.L., Henderson, R.A., Hunt, D.F., Engelhard, V.H., 1993. Recognition of human melanoma cells by HLA-A2.1-restricted cytotoxic T lymphocytes is mediated by at least six shared peptide epitopes. J. Immunol. 150, 2955–2963.

Sosman, J.A., Kim, K.B., Schuchter, L., Gonzalez, R., Pavlick, A.C., Weber, J.S., McArthur, G.A., Hutson, T.E., Moschos, S.J., Flaherty, K.T., et al., 2012. Survival in BRAF V600-mutant advanced melanoma treated with vemurafenib. N. Engl. J. Med. 366, 707–714.

Soucy, T.A., Smith, P.G., Milhollen, M.A., Berger, A.J., Gavin, J.M., Adhikari, S., Brownell, J.E., Burke, K.E., Cardin, D.P., Critchley, S., et al., 2009. An inhibitor of NEDD8-activating enzyme as a new approach to treat cancer. Nature 458, 732–736.

Talantov, D., Mazumder, A., Yu, J.X., Briggs, T., Jiang, Y., Backus, J., Atkins, D., Wang, Y., 2005. Novel genes associated with malignant melanoma but not benign melanocytic lesions. Clin. Cancer Res. 11, 7234–7242.

Tan, M., Li, H., Sun, Y., 2013. Endothelial deletion of Sag/Rbx2/Roc2 E3 ubiquitin ligase causes embryonic lethality and blocks tumor angiogenesis. Oncogene.

Tardat, M., Brustel, J., Kirsh, O., Lefevbre, C., Callanan, M., Sardet, C., Julien, E., 2010. The histone H4 Lys 20 methyltransferase PR-Set7 regulates replication origins in mammalian cells. Nat. Cell Biol. 12, 1086–1093.

Taylor, B.S., Schultz, N., Hieronymus, H., Gopalan, A., Xiao, Y., Carver, B.S., Arora, V.K., Kaushik, P., Cerami, E., Reva, B., et al., 2010. Integrative genomic profiling of human prostate cancer. Cancer Cell 18, 11–22.

Tsai, J., Lee, J.T., Wang, W., Zhang, J., Cho, H., Mamo, S., Bremer, R., Gillette, S., Kong, J., Haass, N.K., et al., 2008. Discovery of a selective inhibitor of oncogenic B-Raf kinase with potent antimelanoma activity. Proc. Natl. Acad. Sci. U. S. A. 105, 3041–3046.

Wei, D., Li, H., Yu, J., Sebolt, J.T., Zhao, L., Lawrence, T.S., Smith, P.G., Morgan, M.A., Sun, Y., 2012. Radiosensitization of human pancreatic cancer cells by MLN4924, an investigational NEDD8-activating enzyme inhibitor. Cancer Res. 72, 282–293.

Weinstein, J.N., A., R., Broom, B.M., Wang, W., Verhaak, R.G., McConkey, D., et al., 2014. Comprehensive molecular characterization of urothelial bladder carcinoma. Nature 507, 315–322.

Yamshchikov, G., Thompson, L., Ross, W.G., Galavotti, H., Aquila, W., Deacon, D., Caldwell, J., Patterson, J.W., Hunt, D.F., Slingluff Jr., C.L., 2001. Analysis of a natural immune response against tumor antigens in a melanoma survivor: lessons applicable to clinical trial evaluations. Clin. Cancer Res. 7, 909s–916s.

Yamshchikov, G.V., Mullins, D.W., Chang, C.C., Ogino, T., Thompson, L., Presley, J., Galavotti, H., Aquila, W., Deacon, D., Ross, W., et al., 2005. Sequential immune escape and shifting of T cell responses in a long-term survivor of melanoma. J. Immunol. 174, 6863–6871.

Zhu, W., Depamphilis, M.L., 2009. Selective killing of cancer cells by suppression of geminin activity. Cancer Res. 69, 4870–4877.